AF 61052 - 69 - C - 0040
SR - II.

OCTOBER 1971

Technion Research &
Development Foundation
Haifa, Israel

SCIENTIFIC REPORT No. 2.

EXPERIMENTAL STUDIES ON BUCKLING OF 7075-T6 ALUMINIUM ALLOY INTEGRALLY STRINGER-STIFFENED SHELLS

BY

TANCHUM WELLER
JOSEF SINGER

Department of Aeronautical Engineering
Technion — Israel Institute of Techn[illegible]gy,
Haifa, Israel

TAE REPORT No. 135

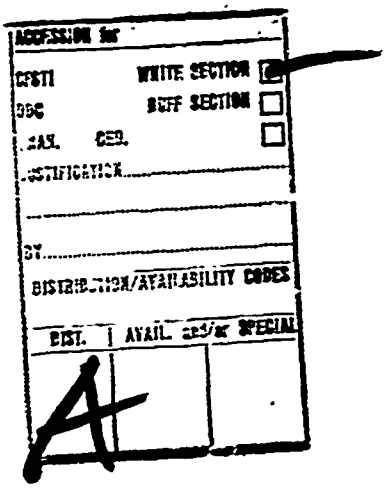

DOCUMENT CONTROL DATA - R & D

(Security classification of title, body of abstract and indexing annotation must be entered when the overall report is classified)

1. ORIGINATING ACTIVITY (Corporate author)
TECHNION RESEARCH AND DEVELOPMENT FOUNDATION
DEPARTMENT OF AERONAUTICAL ENGINEERING
HAIFA, ISRAEL

2a. REPORT SECURITY CLASSIFICATION
UNCLASSIFIED

2b. GROUP

3. REPORT TITLE

EXPERIMENTAL STUDIES ON BUCKLING OF 7075-T6 ALUMINUM ALLOY INTEGRALLY STRINGER-STIFFENED SHELLS

4. DESCRIPTIVE NOTES (Type of report and inclusive dates)
Scientific Interim

5. AUTHOR(S) (First name, middle initial, last name)

TANCHUM WELLER JOSEF SINGER

6. REPORT DATE
Oct 1971

7a. TOTAL NO. OF PAGES
61

7b. NO. OF REFS
30

8a. CONTRACT OR GRANT NO
F61052-69-C-0040

b. PROJECT NO.
9782-01

c.
61102F

d.
681307

9a. ORIGINATOR'S REPORT NUMBER(S)

9b. OTHER REPORT NO(S) (Any other numbers that may be assigned this report)
AFOSR - TR - 72 - 0867

10. DISTRIBUTION STATEMENT
Approved for public release; distribution unlimited.

11. SUPPLEMENTARY NOTES
TECH, OTHER

12. SPONSORING MILITARY ACTIVITY
AF Office of Scientific Research (NAM)
1400 Wilson Boulevard
Arlington, Virginia 22209

13. ABSTRACT

An experimental study of the buckling of closely spaced integrally stringer-stiffened cylindrical shells under axial compression was carried out to determine the influence of shell and stiffener geometry on the applicability of linear shell theory. 38 specimens fabricated from 7075-T6 aluminum alloy with different geometries were tested. Most test specimens were designed to fail in general instability and under low critical stresses to assure elastic buckling. Agreement of experiments with linear theory was found to be governed primarily by the stringer area parameter, (A_1/bh) and the shell geometry parameter, Z. Values of linearity, ρ, (ratio of experimental buckling load to the predicted one) higher than 80% were obtained in the ranges $Z > 1000$ and $(A_1/bh) > 0.5$ and a clear trend towards $\rho = 1$ was observed with increasing values of these parameters. Correlation with linear theory was also found to be influenced by panel unstable postbuckling behavior. No significant effect of other shell and stiffener parameters on the correlation with linear theory could be discerned for the shells tested.

Details of illustrations in this document may be better studied on microfiche

DD FORM 1 NOV 68 1473

UNCLASSIFIED
Security Classification

KEY WORDS	LINK A		LINK B		LINK C	
	ROLE	WT	ROLE	WT	ROLE	WT
7075-T6 STRINGER-STIFFENED CYLINDRICAL SHELLS						
EXPERIMENTAL STUDY OF BUCKLING						
CORRELATION WITH LINEAR THEORY						
INFLUENCE OF STIFFENER AND SHELL GEOMETRY						

F61052-69-C-0040 OCTOBER 1971

SR 2

SCIENTIFIC REPORT No. 2.

EXPERIMENTAL STUDIES ON BUCKLING OF 7075-T6 ALUMINUM ALLOY INTEGRALLY STRINGER-STIFFENED SHELLS

by

TANCHUM WELLER
JOSEF SINGER
Department of Aeronautical Engineering,
Technion - Israel Institute of Technology,
Haifa, Israel.

T.A.E. REPORT No. 135.

The research reported in this document has been sponsored by the Air Force Office of Scientific Research, through the European Office of Aerospace Research, United States Air Force under Contract F61052-69-C-0040.

LIST OF CONTENTS

	PAGE No.
ABSTRACT	I
LIST OF SYMBOLS	II - III
LIST OF FIGURES	IV - VI
1. INTRODUCTION	1 - 4
2. TEST SET-UP AND PROCEDURE	5 - 6
3. TEST SPECIMENS	7 - 9
4. EXPERIMENTAL RESULTS AND DISCUSSION	10 - 17
ACKNOWLEDGEMENT	17
APPENDIX A - THEORETICAL CONSIDERATIONS	18 - 19
REFERENCES	20 - 23
TABLES	24 - 26

ABSTRACT

An experimental study of the buckling of closely spaced integrally stringer-stiffened cylindrical shells under axial compression was carried out to determine the influence of shell and stiffener geometry on the applicability of linear shell theory. 38 specimens fabricated from 7075-T6 aluminum alloy with different geometries were tested. Most test specimens were designed to fail in general instability and under low critical stresses to assure elastic buckling.

Agreement of experiments with linear theory was found to be governed primarily by the stringer area parameter, (A_1/bh) and the shell geometry parameter, Z. Values of linearity, ρ, (ratio of experimental buckling load to the predicted one) higher than 80% were obtained in the ranges $Z > 1000$ and $(A_1/bh) > 0.5$ and a clear trend towards $\rho = 1$ was observed with increasing values of these parameters. Correlation with lineary theory was also found to be influenced by panel unstable postbuckling behavior. No significant effect of other shell and stiffener parameters on the correlation with linear theory could be discerned for the shells tested.

LIST OF SYMBOLS

A_1	cross sectional area of stringers .
b	distance between stringers for a cylindrical shell (see Fig.1).
c, d	the width and height of stringers (see Fig. 1).
D	$Eh^3/12(1 - \nu^2)$.
e_1	eccentricity of stringers (see Fig. 1).
E	modulus of elasticity.
G	shear modulus.
h	thickness of shell.
I_{11}	moment of inertia of stringer cross-section about its centroidal axis.
I_{t1}	torsional constant of stiffener cross section.
K, n	material constants.
L	length of shell between bulkheads.
M_x	moment resultant acting on element.
N_x, $N_{x\phi}$	membrane force resultants acting on element.
n	number of half axial waves in cylindrical shell.
$P_{c\ell}$	classical buckling load for isotropic cylinder for "classical" simple supports (SS3)
P_{cr}	linear theory general instability for stiffened cylinder with "smeared" stiffeners.
P_{exp}	experimental buckling load
P_{South}	critical buckling load computed by "Southwell Slope" method.
R	radius of cylindrical shell, (see Fig. 1)
t	number of circumferential waves.

t_{exp}	experimental number of circumferential waves
u, v, w	non-dimensional displacements, $u = (u^*/R)$, $V = (v^*/R)$, $w = (w^*/R)$ (See Fig. 1).
x^*, z^*, ϕ	axial coordinate along a generator, radial and circumferential coordinates (see Fig. 1).
Z	$= (1 - \nu^2)^{1/2}(L/R)^2(R/h)$ Batdorf shell parameter.
ε_x, ε_ϕ	middle surface strains
γ	$G_1 I_{t1}/bD$
r	structural efficiency
θ	$=[12(1 - \nu^2)]^{1/4}[b/2\pi(Rh)^{1/2}]$ Koiter's measure of total curvature.
λ	$= (PR/\pi D)$ axial compression parameter for cylindrical shell.
ν	Poisson's ratio
ρ	"linearity" $= P_{exp}/P_{cr}$
$\sigma_{y\ 0.1\%}$	stress at 0.1% of strain.
σ_{cr}	critical stress
$(\sigma_{cr})_{n.p.}$	critical stress for a narrow panel Eq. (1A)
$(\sigma_{cr})_{c.c.}$	critical stress for a complete unstiffened cylinder with "classical" simple supports SS3

SS3	simple supports	$v = N_x = w = M_x = 0$
SS4	simple supports	$u = v = w = M_x = 0$
C4	clarped ends	$u = v = w = w_{,x} = 0$

LIST OF FIGURES

FIGURE No.

1 Notation .

2 Test set up.

3 Typical map of gage location .

4 Typical stringer-stiffened specimens .

5 Stress-strain curve of 7075-T6.

6 Set-up for releasing of 7075-T6 specimens .

7 "Linearity" of 7075-T6 stringer-stiffened shells as a function of Z.

8 Effect of unstable panel postbuckling behzvior, $\theta > 0.64$, on "linearity" as a function of Z.

9 "Linearity" of stringer-stiffened shells as a function of Z.

10 Influence of torsional regidity, η_{tl}, on critical loads of stringer stiffened shells.

11 "Linearity" of 7075-T6 and larger steel specimens as a function of Z.

12 "Linearity" of stringer-stiffened shells as a function of Z (excluding results of [20] and [21], smaller steel shells, R = 125 and shells with $\theta > 0.64$)

13 "Linearity" of 7075-T6 and steel (R = 175) stringer-stiffened shells as a function of Z (excluding shells with $\theta > 0.64$).

14 Influence of SS4 Boundary Conditions on the "linearity" of 7075-T6 stringer-stiffened shells.

15 "Linearity" of 7075-T6 stringer-stiffened shells as a function of (A_1/bh).

FIGURE No.

16 Effect of unstable panel postbuckling behaviour, $\theta > 0.64$, on "linearity" as a function (A_1/bh).

17 "Linearity" of stringer-stiffened shells as a function of (A_1/bh).

18 "Linearity" of 7075-T6 and larger steel specimens as a function of (A_1/bh).

19 "Linearity" of stringer-stiffened shells as a function of (A_1/bh) (excluding results of [20] , smaller steel shells, R = 125 and shells with $\theta > 0.64$).

20 "Linearity" of 7075-T6 stringer-stiffened shells as a function of $Z(A_1/bh)$.

21 Effect of unstable panel postbuckling behaviour, $\theta > 0.64$, on the "linearity" as a function of $Z(A_1/bh)$.

22 "Linearity" of 7075-T6 stringer-stiffened shells as a function of "weighted shell geometry" $Z[1 + (A_1/bh)]$

23 Effect of unstable panel postbuckling behavior, $\theta > 0.64$, on "linearity" as a function of $Z[1 + (A_1/bh)]$.

24 SS3 "weighted Linearity" of 7075-T6 stringer stiffened shells.

25 Effect of unstable panel postbuckling behavior, $\theta > 0.64$, on SS3 "weighted Linearity"

26 SS4 "weighted linearity" of 7075-T6 stringer-stiffened shells.

27 Effect of unstable panel postbuckling behavior, $\theta > 0.64$, on SS4 "weighted linearity"

28 "Linearity" of 7075-T6 stringer-stiffened shells as a function of stringer spacing, (b/h).

FIGURE No.

29 "Linearity" of 7075-T6 stringer-stiffened shells as a function of $(b/h)/[1 + (A_1/bh)]$.

30 Structural efficiency of stringer-stiffened shells.

31 Experimental correlation study of imperfection sensitivity dependence on shell geometry Z.

32 Typical circumferential distribution of axial strain (shell AS-14M).

33 Postbuckling patterns of "medium' length specimens.

34 Postbuckling patterns of "long" specimens.

35 Postbuckling patterns of "very long" specimens.

1. INTRODUCTION

In references [1] and [2] the buckling under axial compression of closely spaced integrally stringer-stiffened circular cylindrical shells, was studied experimentally. In these test programs the influence of stiffener and shell geometry on the applicability of linear theory was investigated, as well as the effects of the mechanical properties of shell material. The shells of [1] were fabricated from two different kinds of steel alloys with completely different mechanical properties and those of [2]from 7075-T6 Aluminum alloy. The results of [1] and [2] were correlated with the predicted "classical" linear buckling loads, corresponding to SS3 ($N_x = v = 0$) boundary conditions and with the results of other investigators (for a more complete bibliography see [1] and [2]).

It was shown there that correlation with linear theory predictions was primarily affected by the stringer area-parameter, (A_1/bh), and by shell geometry represented by the Batdorf parameter, Z . For $(A_1/bh) > 0.4$ values of "linearity" (ratio of experimental buckling load to the predicted one) considerably above 60 percents were achieved. Similar results were obtained for $Z > 1000$. For the shorter shells, pre-buckling effects, which are not included in the linear analysis, may be partly responsible for the low buckling loads.

It was also observed in [1] and [2] that the obtained "linearity" was influenced by the stress-strain behavior, or material inelastic

behavior of the shell material as pointed out from theoretical considerations in [3]. Lower values of "linearity" were achieved for shells fabricated from steel with "poor" mechanical properties, that could, however, be corrected if the predicted buckling load was adjusted for the non-linearity of the stress-strain-curve.

The present tests with 7075-T6 stringer-stiffened shells are a continuation of the tests of [1] and [2] for further study of the influence of stiffener and shell-geometry on the adequacy of linear theory predictions. Because of the high yield stress, or rather high ration of $(\sigma_{y.p.}/E)$, of 7075-T6 and the corresponding low buckling stresses of the present test specimens, "inelastic" effects, such as pointed out in [3] should be negligible.

As in the earlier tests, care was taken to load the shells through their mid skin in order to avoid the effect of load eccentricity that can be fairly large (see [4] to [8]).

Local buckling or unstable postbuckling behavior of the cylindrical panels between stringers may also induce low values of "linearity". Koiter's total curvature parameter $\theta = [12(1-\nu^2)]^{1/4}[(b/2\pi)(Rh)^{-1/2}]$, drived in [9] presents a useful criterion for stable postbuckling behavior. For simply supported panels, θ should be less than 0.64 for stable behavior. For stiffer boundaries a slightly larger θ should still be satisfactory. θ can also be taken as a measure of narrowness of the panel which determines the stiffening, within the framework of linear theory, of the panel as compared to a complete cylinder (see [10]).

The local buckling load of the narrow panel should exceed the general instability load to avoid local failure. As an upper bound, the panels may be considered as clamped. Hence, with the aid of approximate methods like [10] and [11] an upper bound for local buckling may be estimated. Therefore, avoiding local buckling and insuring stable postbuckling behavior of the panels is primarily dependent upon proper spacing of the stringers. In [1] the values of θ did rot exceed 0 64, but for some of the shells local buckling of the panels (under assumption of simple supports) was predicted. No definite influence on the "linearity" for these shells could however be discerned in the tests. Some of the specimens of [2] were intentionally designed with $\theta > 0.64$. Local buckling predicted for these specimens could not be detected in the experiments. In the present test program additional shells were designed for further studies of the influence of these factors on the "linearity".

The general instability of the stiffened shells was again calculated with the "smeared" stiffener theory of [12], which does not consider discretness of the stiffeners, an effect found earlier to be usually negligible for closely spaced ring and stringer-stiffened cylinders (see [13] to [15]). The test results in the present program were compared with "classical" SS3 critical loads, as well as loads calculated for the SS4 ($u = v = 0$) boundary conditions.

The "Linearity" of the tested shells depends upon the influence of the initial imperfections. In [1] and [2] correlation of the results with predictions of earlier imperfection sensitivity studies ([7] and [16]) was

attempted. It should be noticed that these investigations are not consistent since [16] predicts extreme sensitivity for externally stringer-stiffened shells in a range of low values of Batdorf geometry parameter, $Z = (1-\nu^2)^{1/2}(L/R)^2(R/h)$, whereas [7] predicts a much less pronounced sensitivity for the same kind of stiffened shells and in a different range of Z. In the tests of [1] and [2] a special effort was made to examine this effect, but it could not be discerned in the experiments. The present test program includes also a further special study of shells in these Z ranges.

Hence the praimary purpose of the present test program is a study of the effect of the combined interaction of shell and stiffeners geometry on the adequacy of "linear" theory in predicting the critical loads for axially compressed stringer-stiffened cylinders and correlation with the results of [1] and [2] and other investigators ([17] to[23]). . .

The present test results like the earlier ones ([1] and [2]) indicate that the dominating stiffener-parameter is the area-parameter, (A_1/bh). For most of the shells with values of $(A_1/bh) > 0.4$ buckling loads of 80 percent and above those predicted by "classical" linear theory were achieved.

2. TEST SET-UP AND PROCEDURE

The test set-up for the present test program is shown in Fig. 2. It is similar to the frame of [1], but smaller in its dimensions and less rigid, because the predicted buckling loads for the present test specimens, which were made of Aluminum alloy, were only about a third of those obtained for the steel specimens of [1] and [2]. Loading manner and procedure as well as specimen mounting is the same as discussed in [1] (for details see Section 4 and Fig. 4 of [1]).

As in [1] and [2] the specimens are not clamped to the supporting discs. They are just located between the lower disc and a similar top disc. The stringers are cut away at both ends of the specimens to ensure that the load is applied at the shell mid-surface and hence to avoid end moments discussed in [4] to [8], (for details see again Section 4 and also Fig. 4 of [1]). The present test boundary conditions are therefore between the SS3 and SS4 boundary conditions (simply supported,

$$w = M_x = 0$$

$$N_x = v = 0 \quad \text{for SS3}$$

and $u = v = 0$ for SS4) and probably nearer to SS4. The restraint to rotation is very small.

About 48 gages were bonded to the surface of each specimen, except for the short shells where a smaller number of gages was used. At least half of the gages were located as close as possible to the edges of the shell. The remaining ones were almost equally distributed over the shell

surface in a manner which enabled correlation of the measurements recorded from these gages, away from the ends of the specimens, and the records from the corresponding gages at the edges. The purpose of the gages at the ends was to study the growth of displacements at the edges in comparison with those away from the edges and hence to obtain information about local effects at the edges and their influence on the experimental critical load. A typical map of gage location is given in Fig. 3, which represents the developed surface of shell AS - 20 #b.

As in [1] and [2], part of the gages were attached axially and the remaining ones circumferentially. The axial gages assisted in confirming elastic behavior up to buckling and adjustments for an even distribution of the applied load, and the circumferential ones were used to detect local bending. All the gages assisted in detection of incipient buckling. Strain-gage readings were recorded on a B & F multichannel strain plotter, and as in [1], [2], [10], [24] to [26] an attempt was made to obtain Southwell plots from the strain records. For this purpose the circumferential gages are more effective (see [1] and [2]).

The specimens were measured carefully at 200-500 points prior to each test. The measuring devices described in [1] and [2] were also used in the present program.

3. TEST SPECIMENS

38 integrally stringer-stiffened shells were tested in the present program. The geometry of the shells is defined in Fig. 1 and their dimensions are presented in Table 1. Some typical specimens are shown in Fig.4.

Most of the specimens were designed to ensure predomination of general instability and elastic buckling. Some were however intensionally designed for unstable postbuckling behavior of the panels between the stringers (see Section 1) in order to verify Koiter's analysis [9] and also study the influence of panel instability on the achieved "linearity". For some of the shells the predicted local buckling predominates and the effect of stiffening on the postbuckling behavior of the panel is studied to obtain a reduced "effective" thickness of a stringer-stiffened shell.

The specimens were machined from 7075-T6 Aluminum alloy tubes (10" in diameter and 1/2" wall thickness) with mechanical properties, that may be approximated by a Ramberg-Osgood stress-strain relation [27]

$$\varepsilon = (\sigma/E) + K(\sigma/E)^n$$

for which

$$E = 0.75 \times 10^4 (Kg/mm^2) = 1.06 \times 10^7 \quad psi$$

$$K = 2.40 \times 10^{56}$$

$$n = 28$$

$$\sigma_{0.1\%} = 54 \ (Kg/mm^2) = 76700 \quad psi$$

The mechanical properties were obtained from specimens cut from the tubes in the axial and circumferential directions and tested in a 20000 lbs. Instron testing machine. The stress-strain curve obtained for these specimens is shown in Fig. 5.

The machining process is similar to that described in [1] and [2], except for mouting of the blank on the mandrel and removing of the finished stiffened shell from it. Here, instead of using the "cooled" mandrel of [1], the blank is carefully heated in a temperature controlled oil bath (Fig. 6) to about 100°C and then mounted on a steel mandrel very similar in its details to the earlier "cooled" mandrel (see Fig. 6). After the cutting process has been completed, the mandrel is located on a special platform within the oil bath, the oil is heated again to 100°C by an electrical heating element within a tube to which the platform is attached. The heated specimen is then released from the mandrel with the aid of a special cylinder which pushes it into the lower part of the oil container (Fig. 6). The bottom of the oil reservoir is padded with rubber to avoid damage of the specimen when it is released from the mandrel. The mandrel is then taken out from the bath and the shell is picked up from the bottom of the container.

The precision of the 7075-T6 specimens did not differ from that obtained for the steel ones of [1] and [2], though they were manufactured from a softer material than the steel alloys used in [1] and [2]. The machining procedure of the present specimens involved the same methods of cutting and measuring and hence the accumulated errors of [1] and [2] were also introduced in the present shells. For the present specimens the worst deviation

in shell thickness for a few shells was up to 10% of the minimum skin thickness. The usual deviation was however within 5% of the minimum thickness.

In order to obtain different values of stringer-distribution, (b/h), stringer-area, (A_1/bh) and Koiter's curvature parameter, θ , special "Form Cutters", were ordered as in [1] and [2]. Four types of cutters are used in the present program: with a cutting surface width of 5mm, 8mm, 10mm, and 12mm. By use of these different cutters together with various division discs, the above mentioned parameters are separately or simultaneously altered.

The aim of the present test program is the study of the effect of shell and stiffener geometry on the obtained "linearity". Hence, the shell parameters (R/h), (L/R) and Z, as well as the stiffener geometry (e_1/h), (A_1/bh), (I_{11}/bh^3) and θ were varied. Many shell configurations were calculated prior to the manufacturing of a specimen to predict the stress levels. To assure elastic buckling the specimens were designed to fail at stresses less than half of the yield strength, ($\sigma_{0.1\%}$) of the material.

As in [1] and [2], "twin" shells were also manufactured in order to study the length effect on imperfection sensitivity found in [7] and [16].

4. EXPERIMENTAL RESULTS AND DISCUSSION

The experimental buckling loads and stresses are given in Table 2. These loads are correllated with the critical loads compared for the SS3 and SS4 boundary conditions, which are also presented in Table 2, to obtain the "linearity" $\rho = (P_{exp}/P_{cr})$. The correlation of experimental results with linear theory for the "classical" SS3 boundary conditions, is presented in Figs. 7 and 8 versus the Batdorf shell parameter Z. In Fig. 14 these results are also compared with those obtained for the SS4 boundary conditions. In Figs. 15 and 16 they are plotted versus the area parameter (A_1/bh), in Figs. 20 and 21 versus the combination $Z(A_1/bh)$, in Fig. 28 versus the stringer distribution (b/h) and in Fig. 29 versus the combination $(b/h)/[1 + (A_1/bh)]$. The different plots represent attempts to identify the dominant geometrical parameters or combination of parameters.

Fig. 7 indicates that the Batdorf shell parameter Z has a considerable influence on the "linearity" obtained, and shows a clear trend towards $\rho = 1$ with increasing values of Z. There is a noticeable scatter of the experimental results, but it can, however, be diminished if Koiter's prediction for unstable panel postbuckling behavior, $\theta > 0.64$, discussed in Section 1 and Appendix A, is considered. Fig. 8 accounts for this behavior, and the shells for which $\theta > 0.64$ are separately identified there. If the experimental results of these shells are excluded, then the effect of Batdorf shell parameter Z, is very pronounced, expecially in the range $Z > 1000$, where the values of "linearity" vary between about 90% and

115%.

In Fig. 9 the results of Figs. 7 and 8 were compared with those of [1] and [2] and other investigations [17] to [23]. It is observed that all the present test results fall within the scatter band of these studies at the corresponding values of Z.

It should be mentioned here that the results of [1] and [2] were too conservative, since upper bound values were taken for the torsional rigidity η_{tl} of the stringers. In [12] it was pointed out that the critical loads of stringer-stiffened shells are affected by the torsional rigidity. This influence is found to be very significant in the range of shell geometry and stiffeners of the present test specimens ($100 < Z < 4000$). Fig. 10 represents this effect for a stringer-configuration, which approximately represents the average of the present specimens. The results of [1] and [2] were corrected by using the exact values of η_{tl} (See[26]).

In Fig.11 the present experimental results are compared with those of [1] and [2] disregarding the results corresponding to the steel specimens, R = 125, for which inelastic effects could be expected. In Fig. 12 the results of the present specimens for which may be suspect of unstable panel postbuckling behavior, since $\theta > 0.64$, were also omitted and the remaining results of Fig. 11 were compared with those of other investigators, except those of [20] and [21]. It can be observed that for high values of $Z(Z > 500)$ the 7075-T6 specimens yield higher values of "linearity" and less scatter. However, it should be pointed out that the results of [19], [22] and [23] are correlated with clamped boundary conditions, and hence are represented more conservatively than the present results. In Fig. 13 the results of [1] for the larger shells

R = 175, and those of the present program for which $\theta < 0.64$ (stable panel behavior) are replotted. The trend towards $\rho = 1$ is very clear there for large values of Z ($Z > 1000$).

In Fig. 14 the experimental results are correlated with the critical load predictions for the SS4 boundary conditions. In the same figure the linearity values for the "classical" SS3 bourdary conditions (shown earlier in Fig.7) are also reproduced. The influence of Z is observed here to be similar to that obtained in Fig. 7, but the SS4 boundary conditions though probably more appropriate to the test conditions, yield lower values of "linearity" which do not approach $\rho = 1$ with increasing values of Z.

Fig. 15 represents the effect of stringer area parameter, (A_1/bh), on the "linearity". As in Fig. 7, scatter of experimental results is quite large, but may be reduced as in Fig. 8, if unstable panel postbuckling behavior is taken into account (see Fig. 16). If the results of Fig. 16 for which $\theta > 0.64$ are excluded, it is found that the values of "linearity" are indeed affected by the stringer area parameter, (A_1/bh). For low values of (A_1/bh) there is still considerable scatter but it diminishes with increasing values of the stringer area parameter and the expected trend to $\rho = 1$ with high (A_1/bh) can be discerned.

In Fig. 17 the present results are compared with the "corrected" ones of [1] and [2] and with those of other studies, [17] to [23]. It appears from this figure that the scatter of the present experimental results is similar to that of other investigations, but the present tests yield higher values of "linearity", ρ . Nevertheless, even with the scatter, a clear

trend towards $\rho = 1$ with increasing values of (A_1/bh) is apparent. In Fig. 18 the small steel specimens, R = 125 of [1] (which is affected by material non-linear behavior) were omitted and the scatter was reduced. In Fig. 19, as in Fig. 12, the present results for which $\theta > 0.64$ were also disregarded and the results were compared with the other investigations mentioned above, except [20]. This figure, like Fig. 13, resutlted in less scatter and a clearer trend to approach $\rho = 1$ with increasing values of (A_1/bh). Beyond $A_1/bh > 0.5$ the values of "linearity" are all above 70%. It appears from this fugure that the experimental resuls of [1], [2] and the present tests yielded higher values of "linearity" than other studies did, but the remark about conservative representation made in regard to Fig. 12 applies also here.

The above discussion indicates that the shell geometry parameter Z and the stringer area parameter (A_1/bh) influence the "linearity", but the scatter of experimental results is considerable. In order to diminish this scatter observed in Figs. 7 and 15 combination of these two parameters was attempted. The "linearity" is therefore plotted versus the combination $Z(A_1/bh)$ in Figs. 20 and 21. In Fig. 21 unstable panel postbuckling behavior was again taken into account. If the shells for which $\theta > 0.64$ are excluded from this figure the scatter of results is noticeably reduced, compared to Fig. 20 and the trend towards $\rho = 1$ is even clearer than that in Fig. 8.

Another attempt to reduce the scatter of the results is made in Figs. 22 and 23, where the "linearity" is represented versus the "weighted shell geometry parameter" $Z[1 + (A_1/bh)]$. The scatter in Fig. 22 is still considerable and similar to that in Fig. 20, but can again be diminished noticeably by taking unstable panel postbuckling behavior into account, as in

Fig. 23. The representation of Fig. 23 is very similar to that of Fig. 21 and hence the scatter band of experimental results is also similar. A clear trend towards $\rho = 1$ with increasing values of $Z[1 + (A_1/bh)]$, can however be seen here, as in Fig. 21.

In Figs. 24 and 25 the "weighted linearity" $\rho_{SS3}/[1 + (A_1/bh)]$ is plotted versus Z. Scatter of results is still appreciable in Fig. 24, but is again diminished in Fig. 25 where unstable panel postbuckling behavior is taken into account and clear trend of increasing "weighted linearity" with increasing values of Z is revealed. In Figs. 26 and 27 the "weighted linearity" is presented for the SS4 boundary conditions. The results of Figs. 26 and 27 are similar to those of Figs. 24 and 25, but with less scatter. Note, that in Figs. 26 and 27 the "weighted linearity" correlated with predictions for SS4 boundary conditions appears to be independent of Z!

In Fig. 28 the influence of stringer-distribution, (b/h), on the "linearity" is studied, but no clear trend is apparent. Similar conclusions were drawin in [1] and [2].

No trend can also be discerned if instead versus (b/h), the "linearity" is plotted versus the comibination $(b/h)/[1 + A_1/bh)]$, as in Fig. 29. In Fig. 30 the structural efficiency η was computed with Eq. (4) of [1]. It is observed that all the stiffened shells tested are more efficient than the "equivalent weight" isotropic shells. Similar results were obtained in [1] and [2]. Hence, in the range of stiffeners of the present investigation the superiority of stiffened shells is clearly verified.

Fig. 31 shows an attempt to evaluate experimentally the results of imperfection sensitivity studies. In these studies, [7] and [16] , the imperfection sensitivity was predicted to be strongly dependent upon the Batdorf parameter Z of the shell. Neither the prediction of [7] or [16] were confirmed. However, the trend towards higher value of ρ with increasing values of Z, appears again. This trend may be due to larger imperfection sensitivity of short shells (or rather shells with low Z), or due to the effect of prebuckling deformations which may be large for short shells (see for example [29]). To clarify this point a non-linear analysis (as in [4] to [8], [14] and [16]) will be applied at a later date.

A typical circumferential distribution of the axial applied load for various stages of loading is shown in Fig. 32 for shell No. AS-14M. The variation in load distribution is similar to that discussed in [1] and [2] and of the same order (about ± 10%) of the average. Most of this non-uniformity is attributed to local thickness variations.

In Figs. 33 to 35 some typical postbuckling patterns are shown for shells of various lengths. As can be seen from these figures the patterns are characterized by two or more tiers of diamonds. However, in the cases of the longest shells tested (Fig. 35), a non-uniform pattern was obtained in some of the shells, like in shells AS-3L or AS-9L, probably due to variations in shell thickness or a non-uniform load distribution. In the other specimens, the patterns show evenly distributed diamonds in the circumferential and axial directions.

The attempt to apply the modified Southwell method of [24] did not yield any better results than in the earlier work([1] and [2]). The critical loads obtained varied between values which were lower than the experimental ones and higher than the ones predicted for the perfect shell. Hence, the scatter of results was found to be even more pronounced for the present specimens than for those of [1] and [2] and the method was again found to be unreliable.

In Table 2 the calculated critical stresses are also given. It can be seen from this Table that these stresses are very low compared with $\sigma_{0.1\%}$ of the shell material. Table 2 also includes the critical local stresses discussed in Section 1 and Appendix A. These calculations indicate that most of the shells failed in a general instability mode. Only for five shells a likelihood of local buckling was identified and the local buckling predictions for these shells are underlined in Table 2. It should however be noticed that the local buckling predictions are calculated for the clamped C4 boundary conditions (see [11]) and so they have to be compared with the predicted instability stresses corresponding to the SS4 boundary conditions. Such a comparison is also given in Table 2 and it can be seen there that local buckling is then predicted for ten of the tested shells. It should be remembered that local buckling predictions were approximated by Eq. (1A) of Appendix A to account for strengthening of the panel due to its narrowness and by [11]. If Eq. (1A) of Appendix A and the results of [30] are compared, it is found that the results of [30] are higher than those obtained by Eq.(1A). On the other hand the results of [11] and [30] coincides. Hence, if local buckling is estimated by [30], which is a more accurate prediction rather than by Eq. (1A),

local buckling is found only for 4 shells (20Ma, 20Mb, 21S and 25S). These results are also given in Table 2.

In [1] it was reasoned that the low values of "linearity" obtained for some of the steel shells with R = 5" were probably due to inelastic effects. This influence was studied by Wesenberg and Mayers for a few shells of [1] and was indeed found to be significant. The inelastic effect "correction" is shown in Table 3.

ACKNOWLEDGEMENT

The authors would like to thank the staff and students of the Aircraft Structures Laboratory of the Department of Aeronautical Engineering for their assistance during the course of the tests, to Mrs. L. Spector and Mrs.M. Gerabli for their assistance with the computations, to Mrs. D. Zirkin for typing of the manuscript and Mr. A. Greenwald for preparing the figures.

APPENDIX A - THEORETICAL CONSIDERATIONS

Failure of stringer-stiffened shells may occur either by general instability of the stiffened shell as a whole or by local buckling of the panels between the stringers. General instability in an axisymmetric buckling mode will occur only for short shells. Therefore, this mode of failure has to be considered only for short stringer stiffened shells or for shells stiffened also with strong rings. The calculations and most of the experimental results of [1] and [2] indicated that the "longitudinal" n = 1 asymmetric buckling mode, pointed out in [20], usually dominates, as it also did in the present test series.

The stringers will appreciably affect the local buckling by their torsional and lateral restraints and there will be an interaction between local and general instability. In an elementary analysis, however, local buckling and general instability are considered separately.

The general instability of stiffened cylindrical shells under axial compression was analysed in [12]. The analysis considers the stiffeners as being "smeared" over the entire length of the shell in a manner which accounts for their eccentricity, (e/h). Ref. [12] is only a solution for the "classical" simply supported SS3 boundary conditions: $w = M_x = v = N_x = 0$ and clamped RF2 boundary conditions: $w = w_{,x} = v = N_x = 0$. An improved analysis which considers all possible combinations of simply supported stringer-stiffened shells is given in [2] and the present test results are correlated with the results of [2] and [12] .

Koiter, in [9], studied the buckling and initial post-buckling behavior of cylindrical panels for stringers imposing no rotational restraint on the panel. The influence of stiffening of the panel due to its narrowness was also shown in [10] to be

$$\frac{(\sigma_{cr})_{n.p.}}{[(\sigma_{cr})_{c.c.}]_{unstiff.}} = (1/2)[(1/\theta^2) + \theta^2] \qquad (1A)$$

where θ is defined by

$$\theta = (1/2\pi)[12(1 - \nu^2)]^{1/4}[b/(Rh)^{1/2}] \quad .$$

Koiter [9] found that transition from "stable plate type" behavior to "unstable cylindrical shell type" occurs at $\theta \approx 0.64$. This value of θ, is however, conservative as the analysis of [9] neglects the torsional constraint. Eq. (1A) is also conservative, since the stringers at the boundaries of the panels impose elastic restraints, which in many cases are close to clamping. Hence, an upper bound for local buckling may be estimated if, for example, Eq. (1A) is corrected by a factor taken from Fig. 1 of [11], which considers complete clamping

REFERENCES

1. Weller, T., Singer, J., and Nachmani, S., "Recent Experimental Studies on the Buckling of Stringer-Stiffened Cylindrical Shells", TAE Report No. 100, Technion Research and Development Foundation, Haifa, Israel, April 1970.

2. Weller, T., "An Experimental and Theoretical Study of Buckling under Axial Compression of Stiffened Cylindrical Shells", D.Sc. Thesis, Technion-Israel Institute of Technology, Haifa, Feb. 1971 (in Hebrew).

3. Wesenberg, D.L., and Mayers, J., "Failure Analysis of Intially Imperfect, Axially Compressed, Orthotropic, Sandwich and Eccentrically Stiffened, Circular Cylindrical Shells", USAAVLABS Technical Report No. 69-86, Dec. 1969.

4. De Luzio, A., Stuhlman, C.E., and Almroth, B., "Influence of Stiffener Eccentricity and End Moment on Stability of Cylinders in Compression", AIAA Journal, 4, (1966), 872-877.

5. Block, D.L., "Influence of Prebuckling Deformation, Ring Stiffeners and Load Eccentricity on the Buckling of Stiffened Cylinders" Presented at the AIAA/ASME 8th Structures, Structural Dynamics and Materials Conference, Palm Springs, California, March 29-31, 1967.

6. Seggelke, P., and Geier, B. "Das BeulverhaltenVerstifter Zylinderschalen", Zeitschrift fur Flugwisenschaften, 15, (1967), 477-490.

7. Hutchinson, J.W., and Frauenthal, J.C., "Elastic Postbuckling Behavior of Stiffened and Barreled Cylinders". J. of Appl. Mech., 36, Series E, (1969) 784-790.

8. Chang, L.K., and Card, M.F., "Thermal Buckling Analysis for Stiffened Orthotropic Cylindrical Shells", NASA TN D-6332, April, 1971.

9. Koiter, W.T., Buckling and Post-Buckling Behavior of a Cylindrical Panel under Axial Compression", Report S.476, National Luchtvaartlaboratorium, Amsterdam, Reports and Transactions, 20, 1956.

10. Singer, J., "The Influence of Stiffener Geometry and Spacing on the Buckling of Axially Compressed Cylindrical and Conical Shells", presented at IUTAM Symposium on Theory of Thin Shells, Copenhagen 1967, pp.234-263. Also TAE Report No. 68, Technion Research and Development Foundation, Haifa, Israel, Oct. 1967.

11. Leggett, D.M.A., "The Buckling of a Long Curved Panel under Axial Compression, R & M No. 1899, A.R.C. Technical Report, July 1942.

12. Singer, J., Baruch, M., and Harari, O., "On the Stability of Eccentrically Stiffened Cylindrical Shells under Axial Compression", International Journal of Solids and Structures 3, (1967), 445-470. Also TAE Report No. 44, Technion Research & Development Foundation, Haifa, Israel, December 1965.

13. Singer, J., and Haftka, R., "Buckling of Discretely Ring-Stiffened Cylindrical Shells", Israel J. of Technology, 6, (1968) 125-137. Also TAE Report No. 67, Technion Research & Development Foundation, Haifa, Israel, Aug. 1967.

14. Block, D.L., "Influence of Discrete Ring Stiffeners and Prebuckling Deformations on the Buckling of Eccentrically Stiffened Orthotopic Cylinders, NASA TN D-4283, Jan. 1968.

15. Singer, J., and Haftka, R., "Buckling of Discretely Stringer-Stiffened Cylindrical Shells and Elastically Restrained Panels and Sub-Shells, TAE Report No. 91, Technion Research & Development Foundation, Haifa, Israel (to be published).

16. Hutchinson, J.W., and Amazigo, J.C., "Imperfection-Sensitivity of Eccentrically Stiffened Cylindrical Shells, AIAA Journal, 5, (1967), 392-401.

17. Len'ko, O.N., The Stability of Orthotropic Cylindrical Shells", Raschet Prostranstvennykh Konstruktsii, Issue IV, pp.499-524, Moscow 1958, Translation NASA TT F-9826, July 1963.

18. Peterson, J.P., and Dow, M.B., "Compression Tests on Circular Cylinders Stiffened Longitudinally by Closely Spaced Z - Section Stringers", NASA MEMO 2-12 59L, 1959.

19. Card, M.F., "Preliminary Results of Compression Tests on Cylinders with Eccentric Longitudinal Stiffeners", NASA TMX-104, September, 1964.

20. Milligan, R., Gerard G., Lakshmikantham, C., and Becker, H., "General Instability of Orthotropic Stiffened Cylinders under Axial Compression", AIAA Journal, 4, (1966), 1906-1913, Also Report Affdl-TR-65-161, Air Force Flight Dynamics Laboratory, USAF, Wright Patterson Air Force Base, Ohio, JUly 1965.

21. Katz, L., "Compression Tests on Integrally Stiffened Cylinders" NASA TMX-55315, August 1965.

22. Card, M.F., and Jones, R.M., "Experimental and Theoretical Results for Buckling of Eccentrically Stiffened Cylinders", NASA TN D-3639, October 1966.

23. Singer, J., Arbocz, J., and Babcock, C.D., Jr. "Buckling of Imperfect Stiffened Cylindrical Shells under Axial Compression" AIAA J., 9 1971, 68-75.

24. Galletly, G.D., and Reynolds, T.E., " A Simpler Extension of Southwell's Method for Determining the Elastic General Instability Pressure for Ring-Stiffened Cylinders Subject to External Hydrostatic Pressure", Proc. Society of Experimental Stress Analysis, 13, 1956, 141-152.

25. Horton, W.H., and Cundari, F.L., "On the Applicability of the Southwell Plot to the Interpretation of Test Data Obtained from Instability Studies of Shell Bodies" SUDAAR No. 290, Department of Aeronautics and Astronautics, Stanford University, August 1966.

26. Tenerelli, D.J., and Horton, W.H., "An Experimental Study of the Local Buckling of Ring-Stiffened Cylinders Subject to Axial Compression, Proc. 11th Annual Conference on Aviation and Astronautics, Israel J. of Tech., 7, March 1969, 181-194.

27. Ramberg, W., and Osgood, W.R., "Description of Stress-Strain Curves by Three Parameters" , NACA Technical Note No. 902, 1943.

28. Timoshenko, S., and Goodyier, J.N., "Theory of Elasticity", McGraw-Hill Book Co., 1951, 275-278.

29. Almroth, B.O., and Bushnell, D., "Computer Analysis of Various Shells of Revolution", AIAA J., 6, (1968), 1848-1855.

30. Rehfield, L.W., and Hallauer, W.L. Jr., "Edge Restrairt Effect on Buckling of Compressed Curved Panels", AIAA J., 6., (1968), 187-189.

TABLE 1 - Stringer-Stiffened Shells - Dimensions

Shell	L(mm)	h(mm)	R(mm)	R/h	L/R	Z	d(mm)	c(mm)	b(mm)	$-(e_1/h)$	A_1/bh	I_{11}/bh^3	η_{t1}	θ	b/h	$\frac{b/h}{1+(A_1/bh)}$
As-1s	60	.229	120.6	530	.498	120	.757	1.06	9.06	2.15	.387	.352	3.32	.498	39.6	28.5
As-1L	182	.241	120.6	500	1.51	1090	.751	1.06	9.06	2.06	.364	.295	2.79	.486	37.6	27.6
As-2L	290	.240	120.6	500	1.51	1740	.747	1.06	9.06	2.06	.364	.294	2.80	.487	37.8	27.7
As-3L	346	.256	120.6	470	2.87	3700	.764	1.06	9.06	1.99	.349	.259	2.43	.472	35.4	26.2
As-4s	60	.258	120.6	470	.497	110	1.24	1.08	9.08	2.90	.571	1.09	6.67	.471	35.2	22.4
As-4L	175.5	.254	120.6	480	1.47	960	1.25	1.08	9.08	2.97	.586	1.19	7.11	.475	35.7	22.5
As-5L	248	.246	120.6	490	2.06	1980	1.26	1.08	9.08	3.06	.608	1.33	7.91	.482	36.9	22.9
As-6L	315	.265	120.6	460	2.61	2960	1.27	1.08	9.08	2.89	.568	1.08	6.40	.465	34.3	21.9
As-7s	60.5	.261	120.6	560	.502	110	.699	1.19	11.2	1.84	.285	.170	1.82	.577	42.9	33.4
As-7L	182	.256	120.6	470	1.51	1020	.729	1.19	11.2	1.92	.303	.205	2.14	.583	43.7	33.6
As-8L	247.5	.248	120.6	490	2.05	1950	.741	1.19	11.2	1.99	.318	.237	2.53	.592	45.1	34.2
As-9L	345	.261	120.6	460	2.86	3610	.749	1.19	11.2	1.94	.305	.210	2.17	.577	42.9	32.9
As-10L	347	.250	120.6	480	2.88	3810	1.28	1.22	11.2	3.06	.557	1.22	8.19	.591	44.9	28.8
As-11s	61	.262	120.6	460	.506	110	1.23	1.22	11.2	2.84	.508	.926	6.48	.577	42.8	28.4
As-11L	182	.256	120.6	470	1.51	1020	1.25	1.22	11.2	2.94	.531	1.05	7.10	.584	43.8	28.6
As-12L	243	.248	120.6	490	2.02	1880	1.25	1.22	11.2	3.02	.549	1.17	8.03	.594	45.2	29.2
As-13m	123	.240	120.6	500	1.02	500	1.27	1.22	11.2	3.15	.577	1.36	9.15	.603	46.8	29.6
As-14m	114	.244	120.6	490	.945	420	1.25	1.21	11.2	3.06	.553	1.21	8.17	.598	45.9	29.6
As-15s	61	.244	120.6	490	.506	120	.759	1.59	13.6	2.06	.364	.294	3.59	.725	55.7	40.8
As-15L	180	.238	120.6	510	1.49	1080	.774	1.59	13.6	2.13	.381	.335	3.76	.734	57.1	41.4
As-16ma	90.8	.228	120.6	530	.753	290	1.24	1.61	13.6	3.21	.642	1.57	14.1	.751	59.7	36.4
As-16mb	91.9	.239	120.6	510	.762	280	1.23	1.62	13.6	3.07	.613	1.35	12.2	.734	57.0	35.3
As-17ma	90	.236	120.6	510	.746	270	1.27	1.08	9.08	3.18	.637	1.52	8.98	.497	38.5	23.5
As-17mb	89	.237	120.6	510	.748	260	1.28	1.08	9.08	3.20	.642	1.56	9.16	.491	38.3	23.3
As-18ma	122	.235	120.6	510	1.01	500	1.53	1.09	9.09	3.76	.779	2.75	13.2	.494	38.7	21.8
As-18mb	122	.239	120.6	510	1.01	490	1.53	1.09	9.09	3.69	.764	2.59	12.5	.490	38.0	21.5
As-19ma	122	.257	120.6	470	1.01	460	1.47	1.22	11.2	3.37	.628	1.72	9.97	.584	43.7	26.8
As-19mb	122	.240	120.6	500	1.01	490	1.49	1.22	11.2	3.61	.675	2.17	12.3	.603	45.8	27.9
As-20ma	121	.223	120.6	540	1.00	520	1.52	1.63	13.6	3.91	.815	3.16	23.9	.760	61.1	33.9
As-20mb	120	.220	120.6	550	.995	520	1.53	1.63	13.6	3.98	.833	3.37	25.1	.766	62.0	33.8
As-21s	62	.236	120.6	510	.514	130	1.27	1.62	13.6	3.19	.639	1.54	13.5	.739	57.7	35.2
As-21L	180	.240	120.6	500	1.49	1070	1.26	1.62	13.6	3.13	.626	1.44	12.7	.732	56.8	34.9
As-22L	245	.231	120.6	510	2.03	2060	1.29	1.62	13.6	3.27	.659	1.69	14.8	.746	58.9	35.5
As-23L	247	.236	120.6	550	2.05	2040	.743	1.59	13.6	2.07	.369	.305	3.63	.737	57.6	42.3
As-24s	58.1	.218	120.6	550	.482	120	.774	1.59	13.6	2.28	.415	.436	5.08	.767	62.3	44.0
As-24L	300	.227	120.6	530	2.49	3140	.755	1.59	13.6	2.19	.394	.373	4.36	.751	57.6	41.3
As-25s	71.2	.218	120.6	550	.590	180	1.28	1.62	13.6	3.45	.701	2.02	17.7	.768	62.5	36.7
As-25L	302	.215	120.6	560	2.50	3360	1.28	1.62	13.6	3.47	.708	2.09	18.3	.774	63.4	37.1

TABLE 2 - Buckling of Stringer-Stiffened Shell. - Experimental Results and Comparison with Linear Theory

Shell	P_{cr} $(\eta_{t_1}=0)$ (Kg)	P_{cr} $(\eta_{t_1}\neq 0)$ SS3 (Kg)	t	P_{cr} $(\eta_{t_1}\neq 0)$ SS4 (Kg)	t	P_{exp} (Kg)	t_{exp}	$\rho=P_{exp}/P_{cr}$ $(\eta_{t_1}\neq 0)$ SS3	$\rho=P_{exp}/P_{cr}$ $(\eta_{t_1}\neq 0)$ SS4	σ_{cr_2} (Kg/mm^2)	$\frac{(\sigma_{cr})_{n.p.}}{(\sigma_{cr})_{c.c.}}$ eq. (1A)	$\frac{(\sigma_{cr})_{C4}}{(\sigma_{cr})_{SS4}}$ [11]	$\frac{(\sigma_{cr})_{C4}}{(\sigma_{cr})_{c.c.}}$ [11] & eq.(1A)	$\frac{(\sigma_{cr})_{C4}}{(\sigma_{cr})_{c.c.}}$ [30]	$\frac{\sigma_{cr}}{(\sigma_{cr})_{c.c.}}$ stiff. SS3	$\frac{\sigma_{cr}}{(\sigma_{cr})_{c.c.}}$ stiff. SS4	P_{South} (Kg)	η effic.- -iency
AS - 1S	2550	2900	15	3250	16	2020	12	.696	.623	12.1	2.14	1.53	3.27		1.40	1.57	2080	1.54
AS - 1L	2250	2370	9	3030	13	2270	8	.957	.747	9.51	2.24	1.54	3.45		1.05	1.34	2470	1.59
AS - 2L	2200	2280	8	2900	14	2030	7	.887	.698	9.19	2.23	1.54	3.43		1.02	1.30		1.44
AS - 3L	2290	2360	9	2990	12	2420	7	1.03	.809	9.01	2.36	1.53	3.61		.979	1.24		1.51
AS - 4S	4650	5550	14	5750	14	5250	10	.946	.912	18.1	2.37	1.53	3.63		1.86	1.93		2.23
AS - 4L	2890	3270	9	4710	13	3280		1.00	.696	10.7	2.33	1.53	3.56		1.12	1.61		1.41
AS - 5L	2620	2890	8	4180	12	3230		1.12	.772	9.64	2.27	1.54	3.47		1.04	1.50	3240	1.46
AS - 6L	2810	3030	7	4380	10	2970	6	.985	.677	9.59	2.42	1.55	3.70		.96	1.39		1.19
AS - 7S	2720	2970	14	3660	15	2100		.707	.574	11.69	1.76	1.46	2.44		1.19	1.47		1.38
AS - 7L	2320	2420	9	3200	13	2630	11	1.08	.818	9.57	1.64	1.45	2.38		.99	1.31	2890	1.77
AS - 8L	2090	2170	8	2920	13	2540	7	1.17	.870	8.76	1.60	1.45	2.32		.94	1.26	2760	1.81
AS - 9L	2340	2400	7	2990	12	2270	10	.946	.758	9.30	1.67	1.46	2.44		.95	1.19	2340	1.46
AS -10L	2470	2690	7	3930	10	2950	6	1.10	.750	9.12	1.61	1.45	2.33		.97	1.42	3050	1.38
AS -11S	4360	5250	14	5600	14	4740	10	.904	.846	17.53	1.67	1.47	2.45		1.78	1.90	5030	2.14
AS -11L	2830	3180	9	4620	13	3350	9	1.05	.724	10.7	1.64	1.42	2.33		1.11	1.61		1.54
AS -12L	2540	2820	8	4160	12	3260	7	1.16	.783	9.69	1.60	1.39	2.22		1.04	1.53	3330	1.58
AS -13M	2880	3510	11	4590	12	3510	8	1.00	.766	12.2	1.56	1.39	2.17		1.36	1.78		1.72
AS -14M	3280	3460	11	4630	12	3280	9	.947	.672	12.1	1.58	1.46	2.31		1.31	1.75		1.64
AS -15S	2680	3100	15	3630	15	2390	12	.767	.655	12.3	1.22	1.46	1.78		1.34	1.57		1.62
AS -15L	2120	2270	9	3090	13	2510	9	1.11	.812	9.12	1.20	1.44	1.73		1.02	1.39		1.76
AS -16Ma	3080	4100	12	4760	13	2880	11	.703	.605	14.5	1.17	1.44	1.68	2.02	1.68	(1.95)		1.48
AS -16Mb	3240	4220	12	4970	13	3080	10	.729	.619	14.4	1.20	1.44	1.73	1.94	1.61	(1.90)		1.47
AS -17Ma**	3320	4030	13	4700	13	2470	11	.613	.525	13.8	2.19	1.54	3.37		1.55	1.82		1.18
AS -17Mb**	3390	4130	13	4790	13	2200	13	.532	.458	14.6	2.19	1.54	3.37		1.57	1.82		1.03
AS -18Ma	3400	4240	11	5170	12	3710	12	.876	.717	13.4	2.17	1.53	3.32		1.51	1.84		1.47
AS -18Mb	3460	4280	11	5440	12	3410	10	.796	.627	13.4	2.21	1.54	3.40		1.49	1.89		1.32
AS -19Ma*	3590	4460	12	5510	12	2430	10	.543	.439	14.1	1.64	1.45	2.38		1.45	1.79		1.57
AS -19Mb	3270	4070	11	5110	12	3430	9	.842	.669	13.4	1.56	1.42	2.22		1.48	1.86		1.49
AS -20Ma	3180	4460	11	5370	12	3940	9	.884	.734	14.9	1.15	1.27	1.46	1.80***	1.73	(2.08)		1.68
AS -20Mb	3170	4480		5350	12	2990	10	.667	.593	14.7	1.15	1.27	1.46	1.80***	1.77	(2.11)		1.29
AS -21S	4170	5540	14	5780	14	4700	11	.848	.813	18.9	1.19	1.32	1.57	1.86***	2.13	(2.22)		2.23
AS -21L	2650	3240	9	4800	13	3120	8	.963	.653	10.9	1.20	1.31	1.57	1.84	1.21	(1.79)		1.45
AS -22L	2370	2790	8	4230	12	2740	7	.982	.648	9.60	1.18	1.27	1.50	1.79	1.10	(1.67)		1.33
AS -23L	1980	2090	8	2940	13	1500	6	.718	.539	8.53	1.19	1.31	1.56		.96	1.30		1.10
AS -24S	2340	2810	15	3200	16	1910	12	.680	.597	12.0	1.14	1.27	1.45	1.82	1.46	(1.66)		1.56
AS -24L	1890	1990	7	2640	13	1350	6	.678	.511	8.3	1.17	1.43	1.67		.97	1.29		1.03
AS -25S	4050	5540	14	5680	14	3430	11	.619	.604	19.7	1.14	1.27	1.45	1.81***	2.40	(2.46)		1.80
AS -25L	2010	2420	8	3890	9	2230	7	.921	.573	8.7	1.13	1.27	1.44	1.81	1.09	(1.74)		1.20

* local buckling observed in test - not included in discussion

** incorrect experimental load records - not included in discussion

*** local buckling predictions $\left[\frac{(\sigma_{cr})_{C4}}{(\sigma_{cr})_{c.c.}}\right]_{local\ [30]} < \left[\frac{(\sigma_{cr})_{SS4}}{(\sigma_{cr})_{c.c.}}\right]_{stiff.}$

underlined values $\left[\frac{(\sigma_{cr})_{C4}}{(\sigma_{cr})_{c.c.}}\right]_{local\ [11]\ \&\ eq.\ (1A)} < \left[\frac{(\sigma_{cr})_{SS3}}{(\sigma_{cr})_{c.c.}}\right]_{stiff}$

numbers in brackets $\left[\frac{(\sigma_{cr})_{C4}}{(\sigma_{cr})_{c.c.}}\right]_{local\ [11]\ \&\ eq.\ (1A)} < \left[\frac{(\sigma_{cr})_{SS4}}{(\sigma_{cr})_{c.c.}}\right]_{stiff}$

(See page 16)

TABLE 3: Influence of Inelastic Behavior of Shell Material on the "Linearity"

Shell*	$\rho = P_{exp}/P_{cr}$ SS3 [1] & [2]	inelastic correction ρ [3]
SZ - 3 **	0.672	0.789
7 - L **	0.699	0.855
13 - L ***	0.901	0.901
24 - L ***	0.756	0.756

* Steel alloy stringer-stiffened shells of [1] & [2].

** R = 5"

*** R = 7"

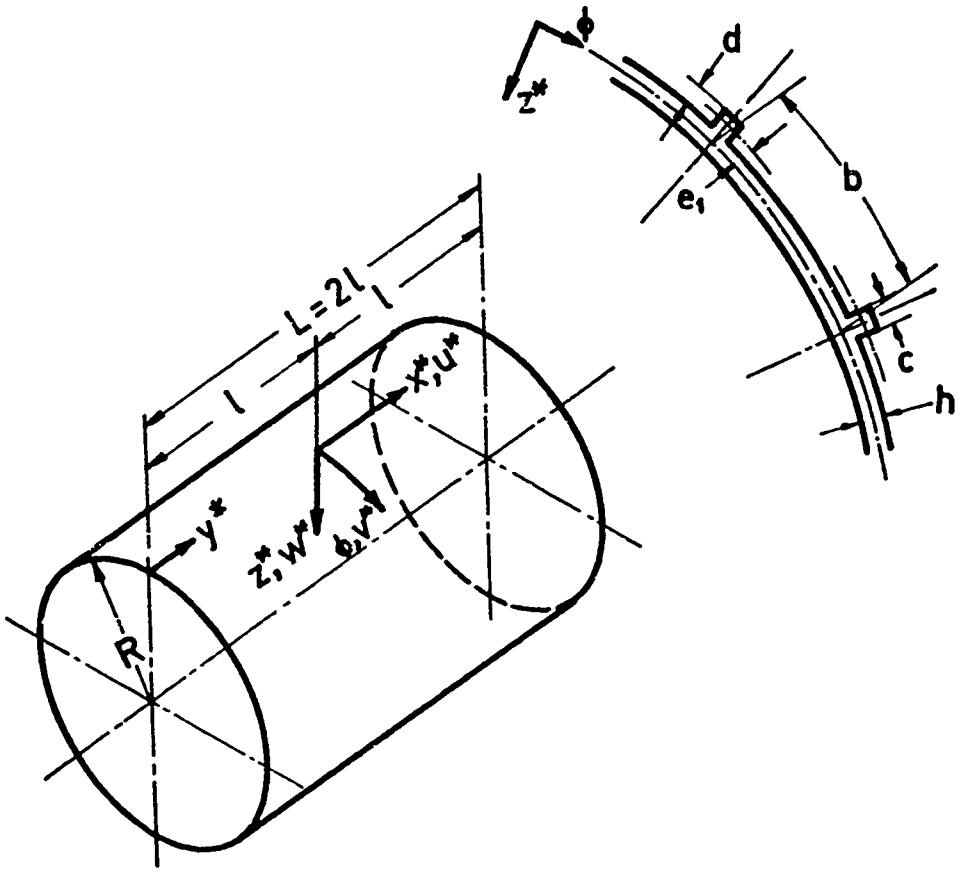

FIG. 1 NOTATION

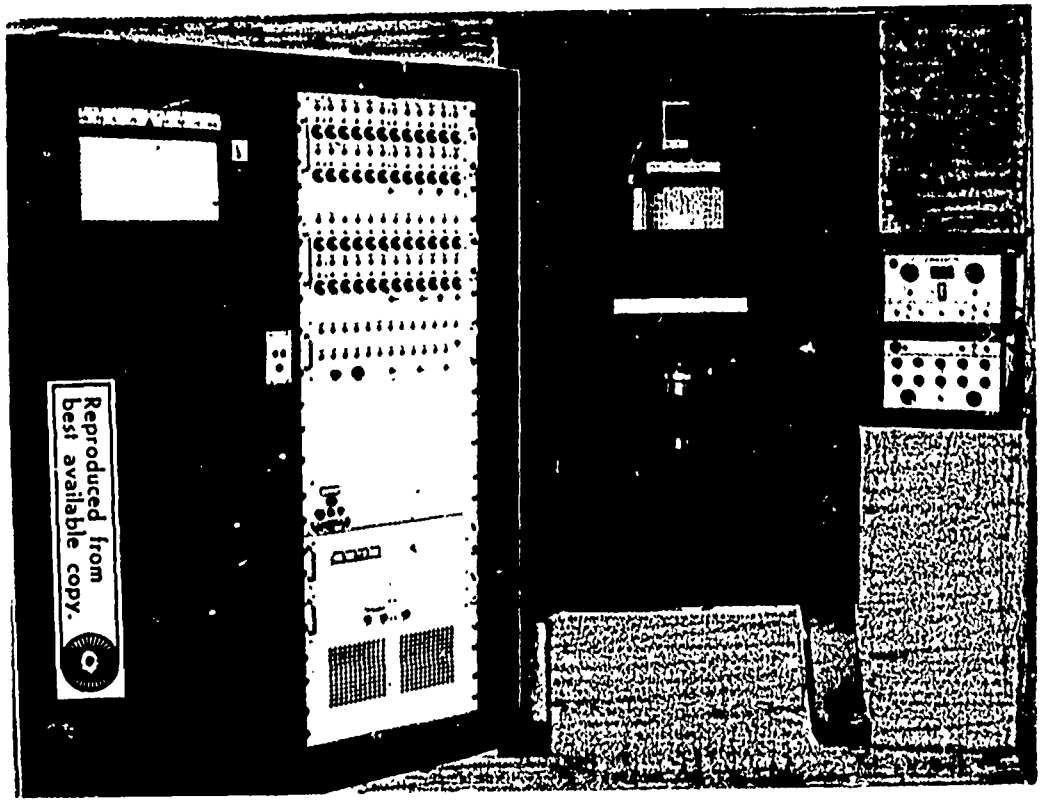

FIG. 2 TEST SET-UP

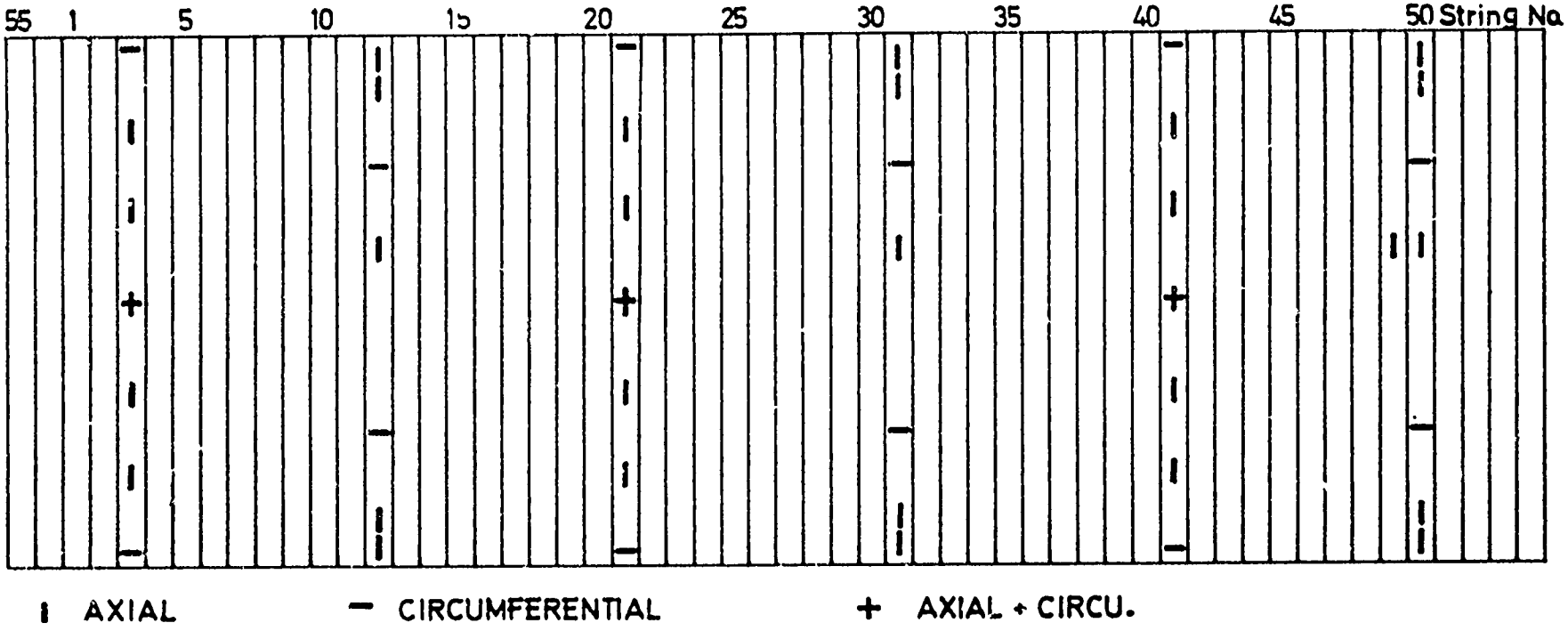

TYPICAL MAP OF CAGE LOCATED (DEVELOPED SURFACE OF SHELL AS-20 Mb)

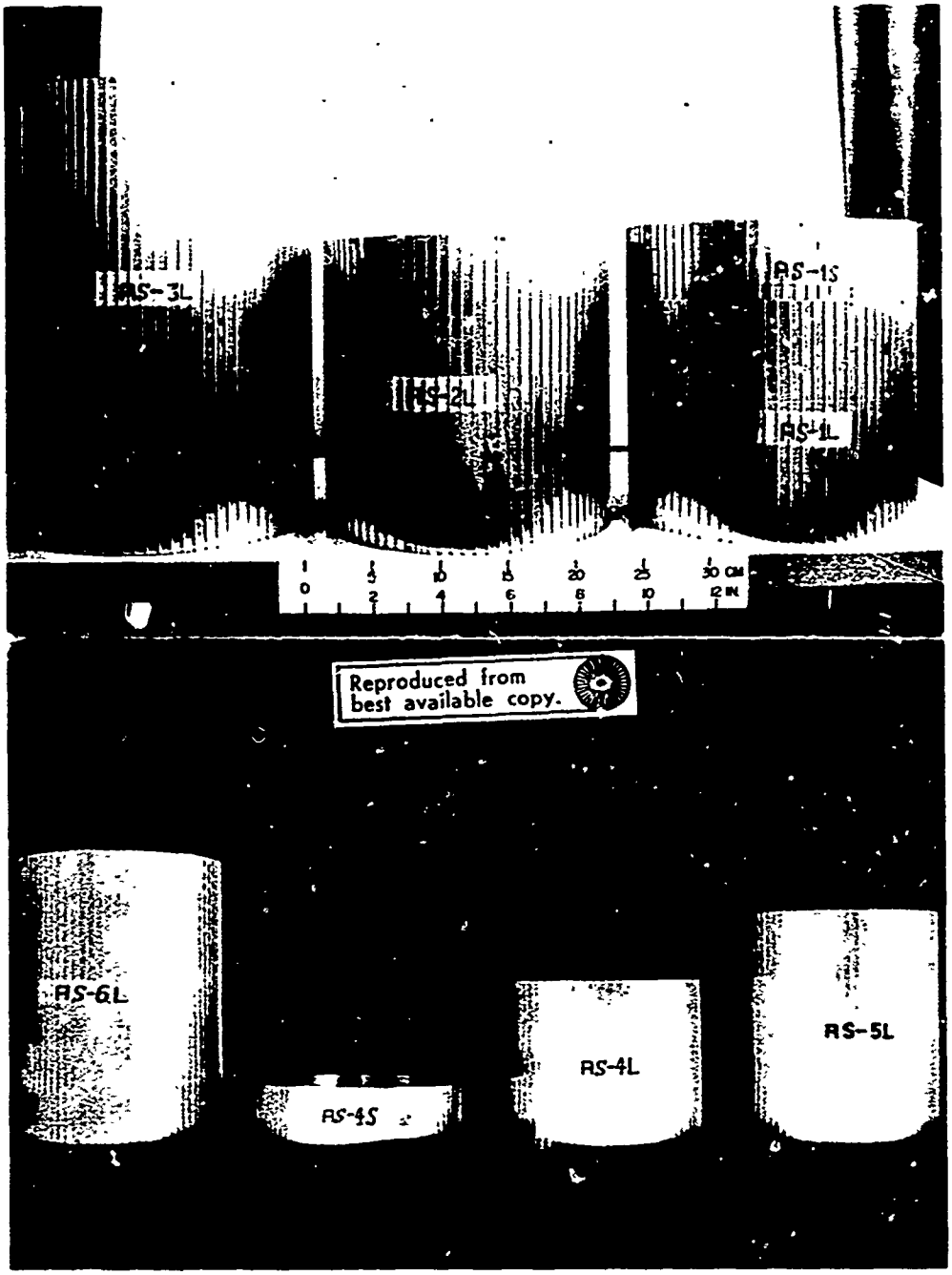

FIG. 4. TYPICAL STRINGER-STIFFENED SPECIMENS

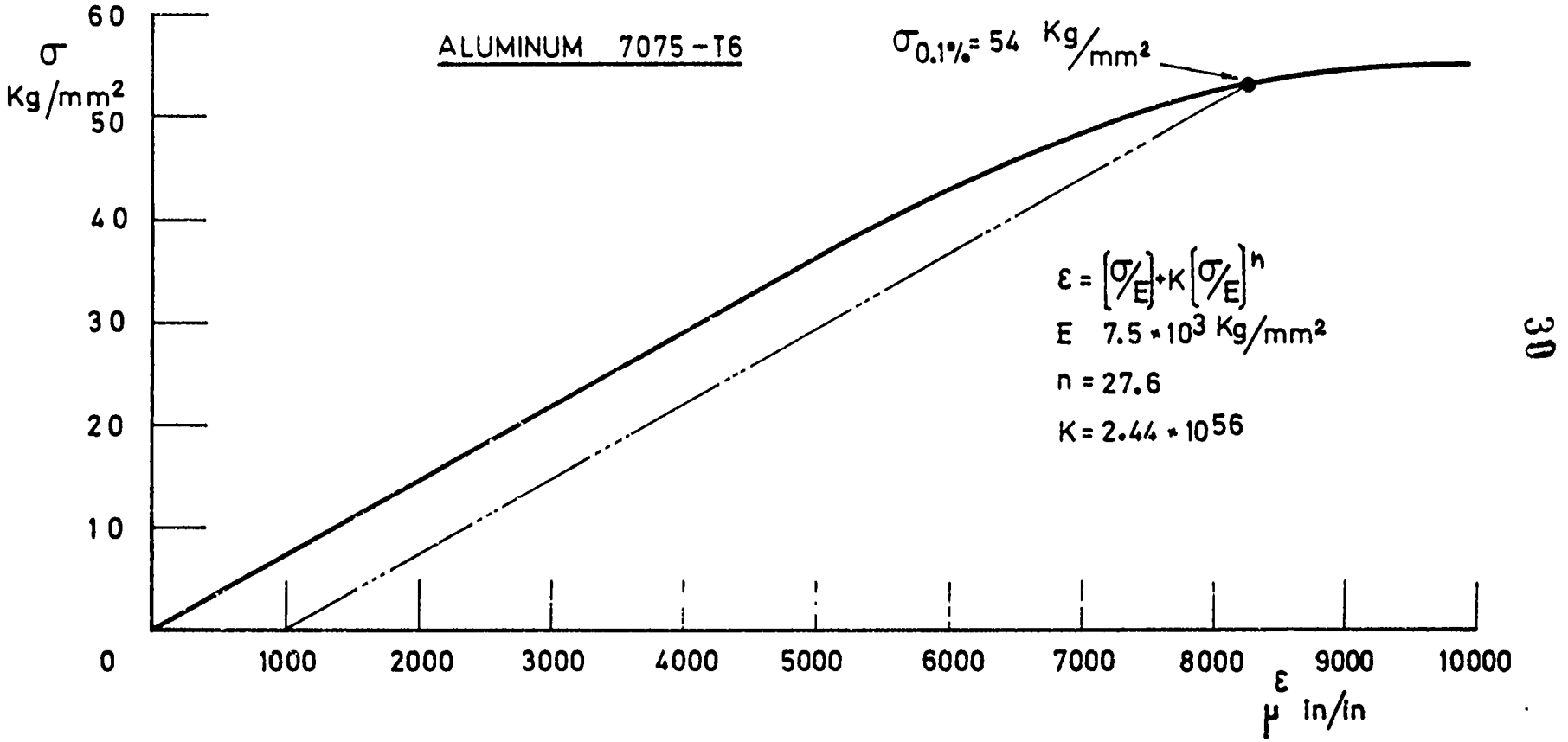

FIG. 5. STRESS-STRAIN CURVE OF 7075-T6

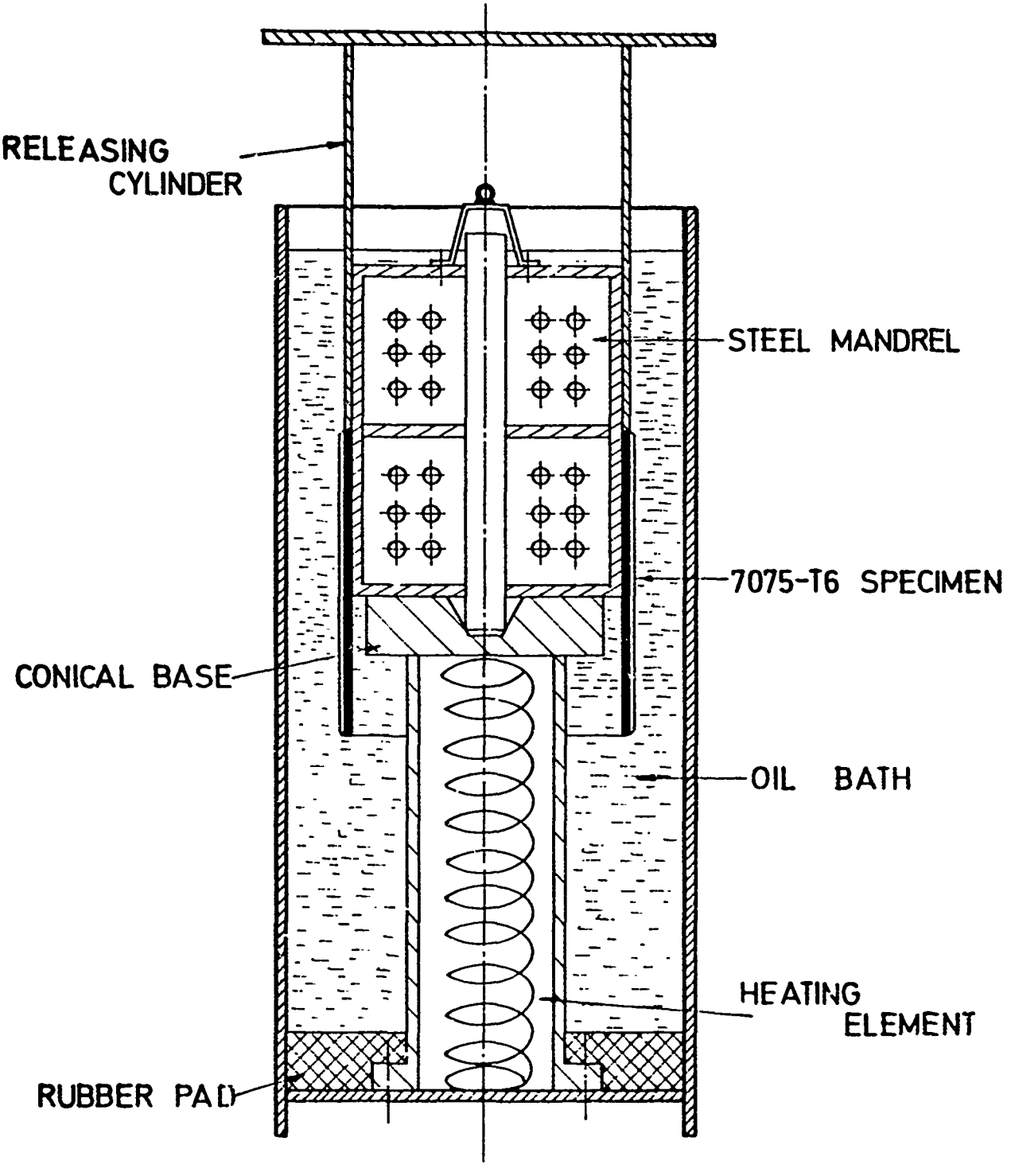

FIG. 6. SET-UP FOR RELEASING OF 7075-T6 SPECIMENS

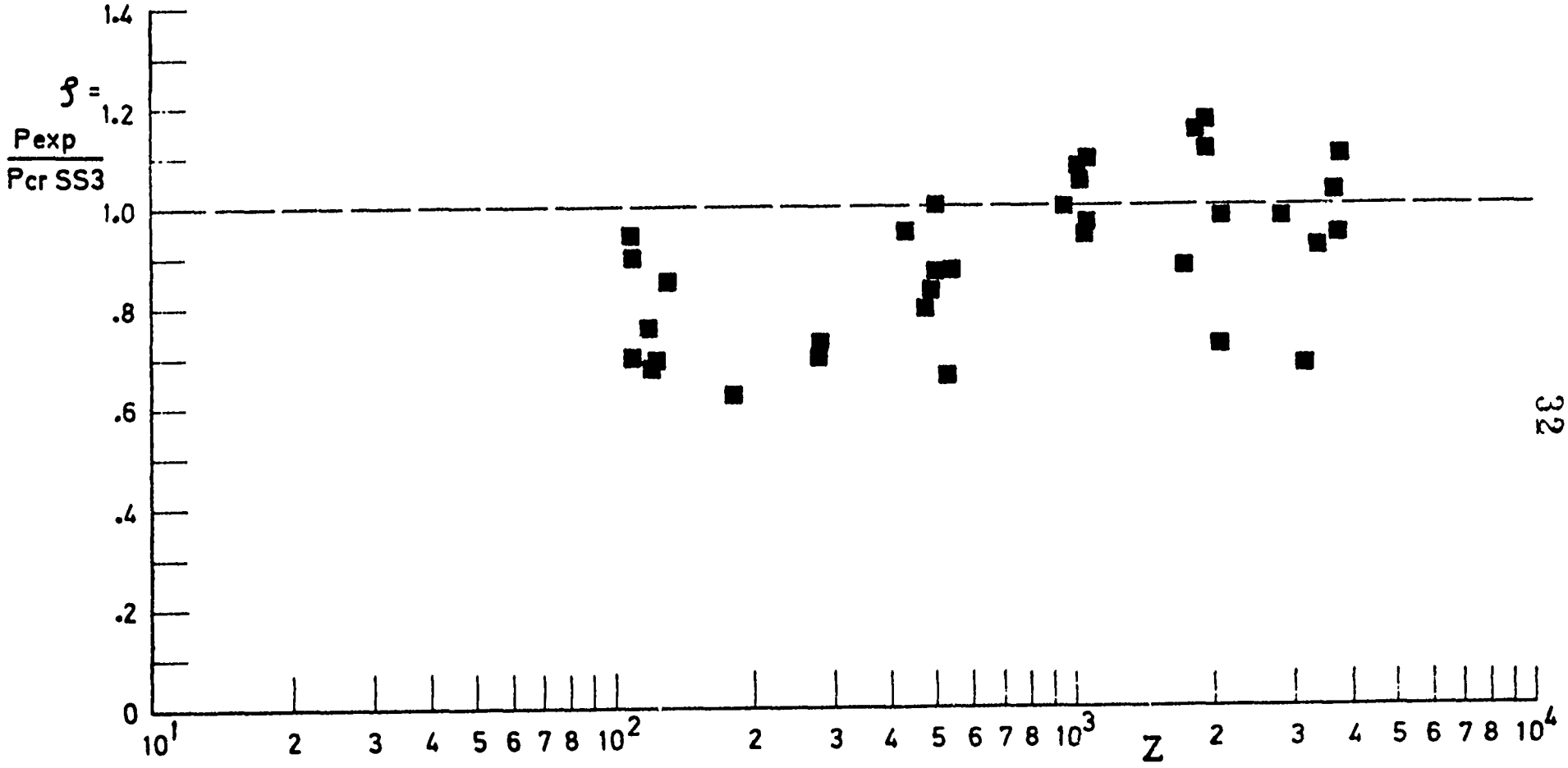

FIG. 7. "LINEARITY" OF 7075-T6 STRINGER-STIFFENED SHELLS AS A FUNCTION OF Z

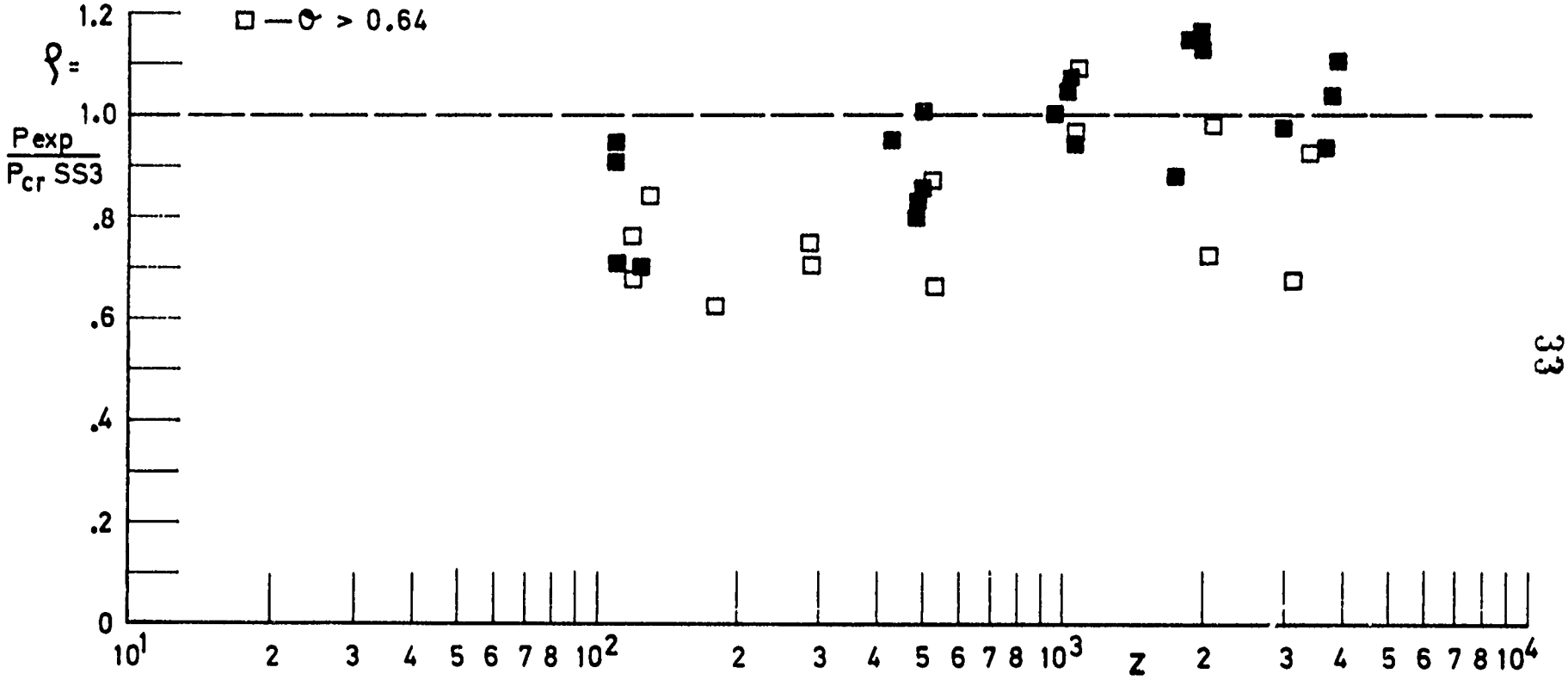

FIG. 8. EFFECT OF UNSTABLE PANEL POSTBUCKLING BEHAVIOR, σ>0.64, ON "LINEARITY" AS A FUNCTION OF Z

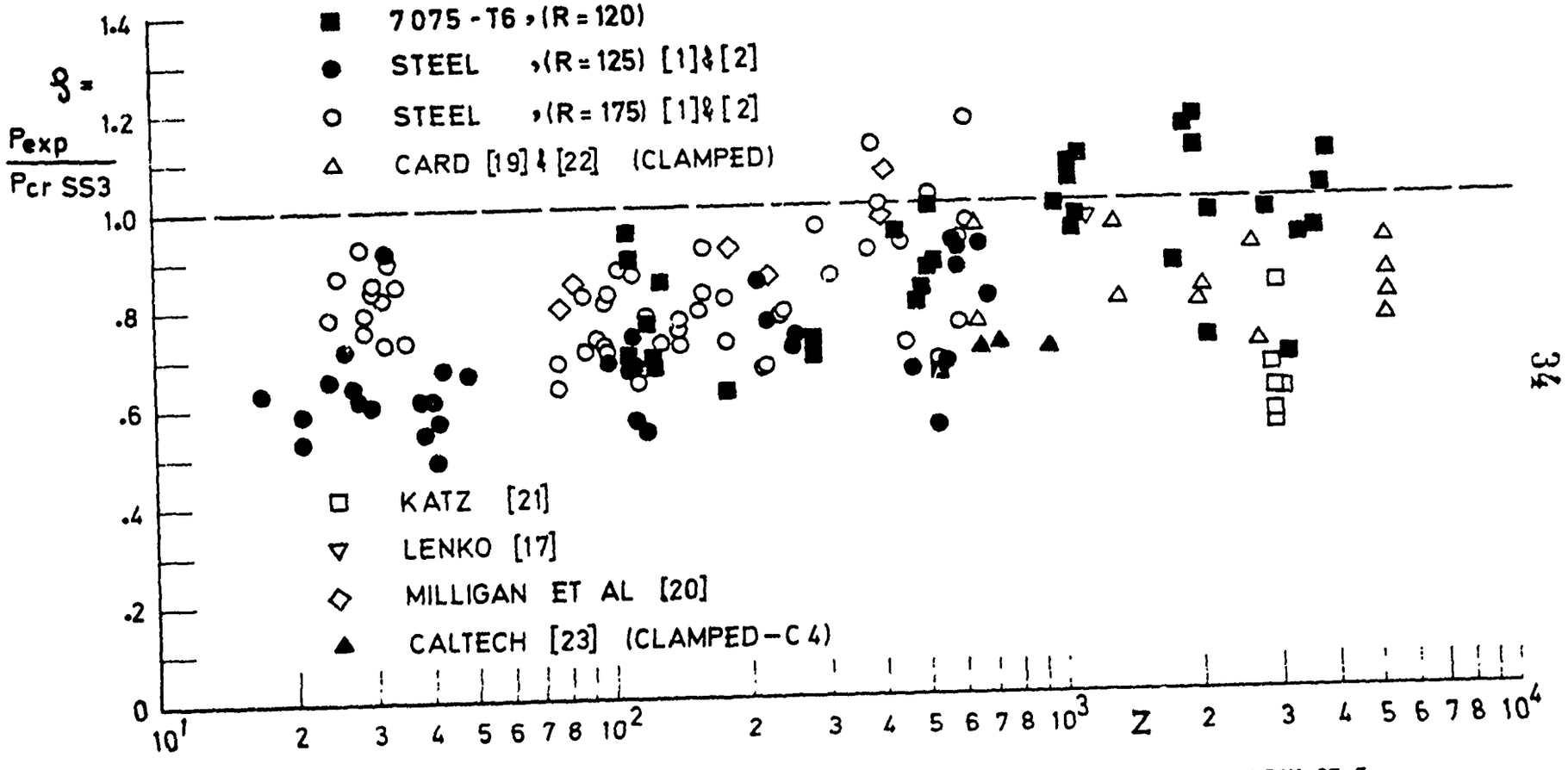

FIG. 9. "LINEARITY" OF STRINGER-STIFFENED SHELLS AS A FUNCTION OF Z

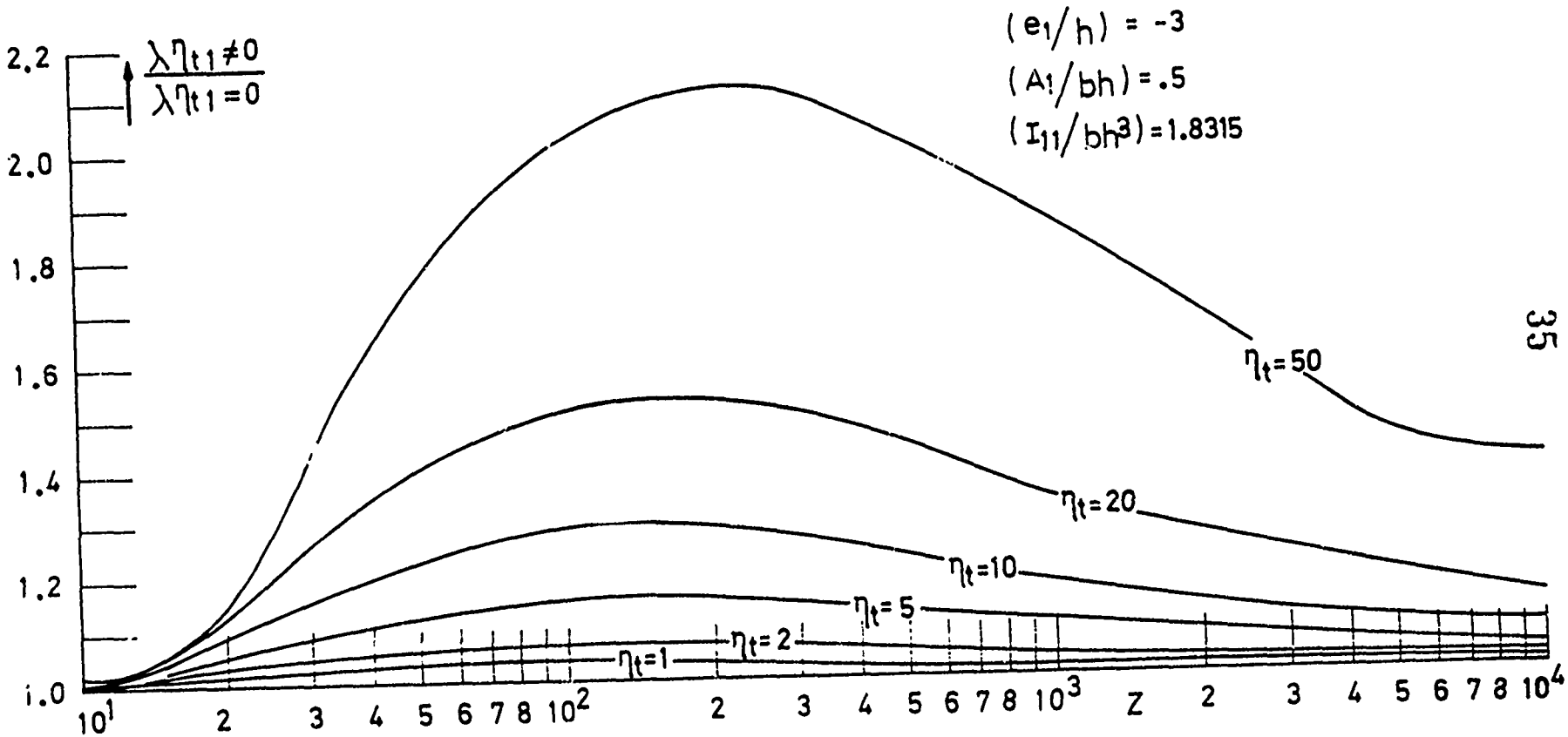

FIG. 10. INFLUENCE OF TORSIONAL RIGIDITY, η_{t1}, ON CRITICAL LOADS OF STRINGER-STIFFENED SHELLS

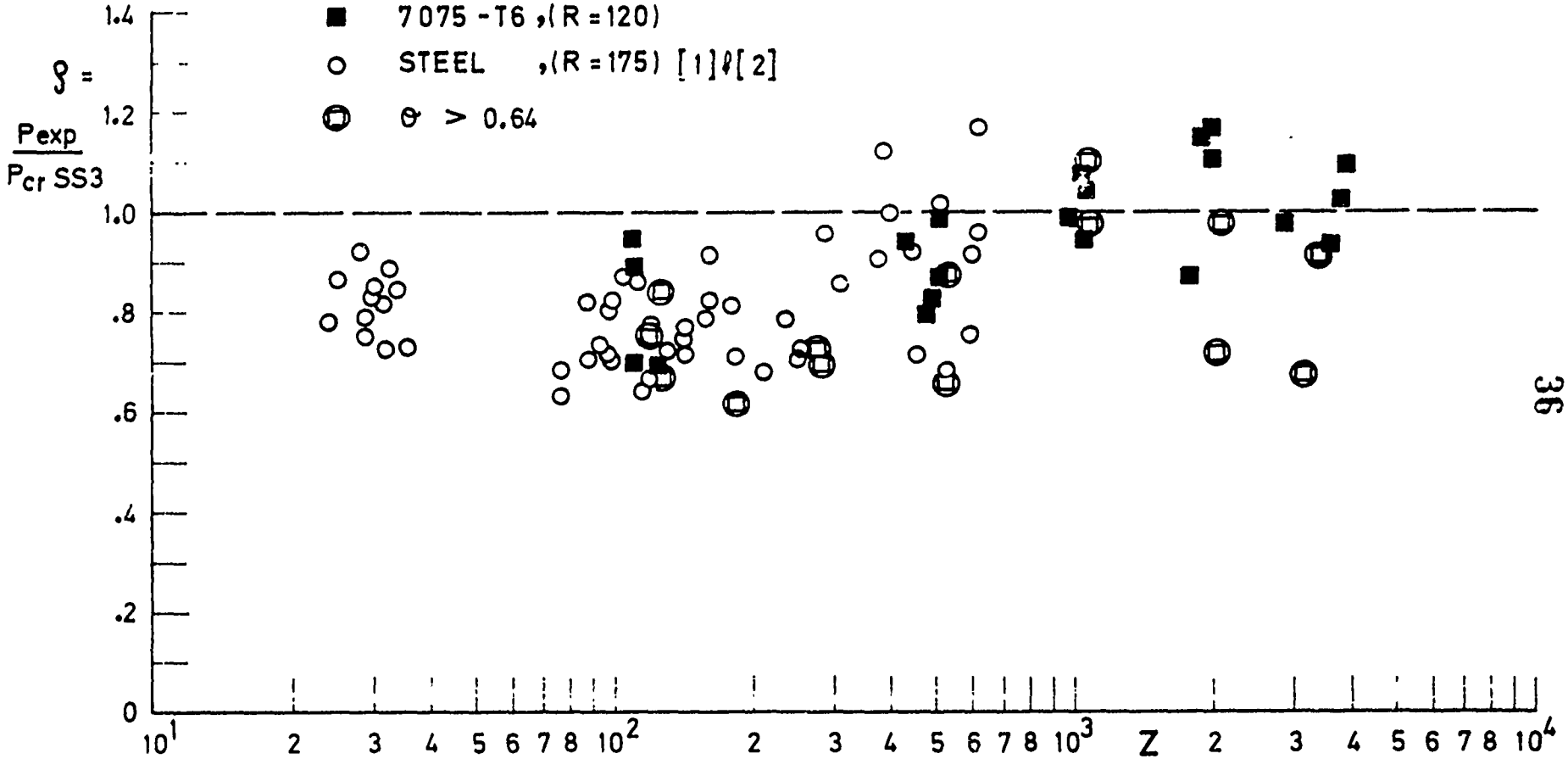

FIG. 11. "LINEARITY" OF 7075-T6 AND LARGER STEEL SPECIMENS AS A FUNCTION OF Z

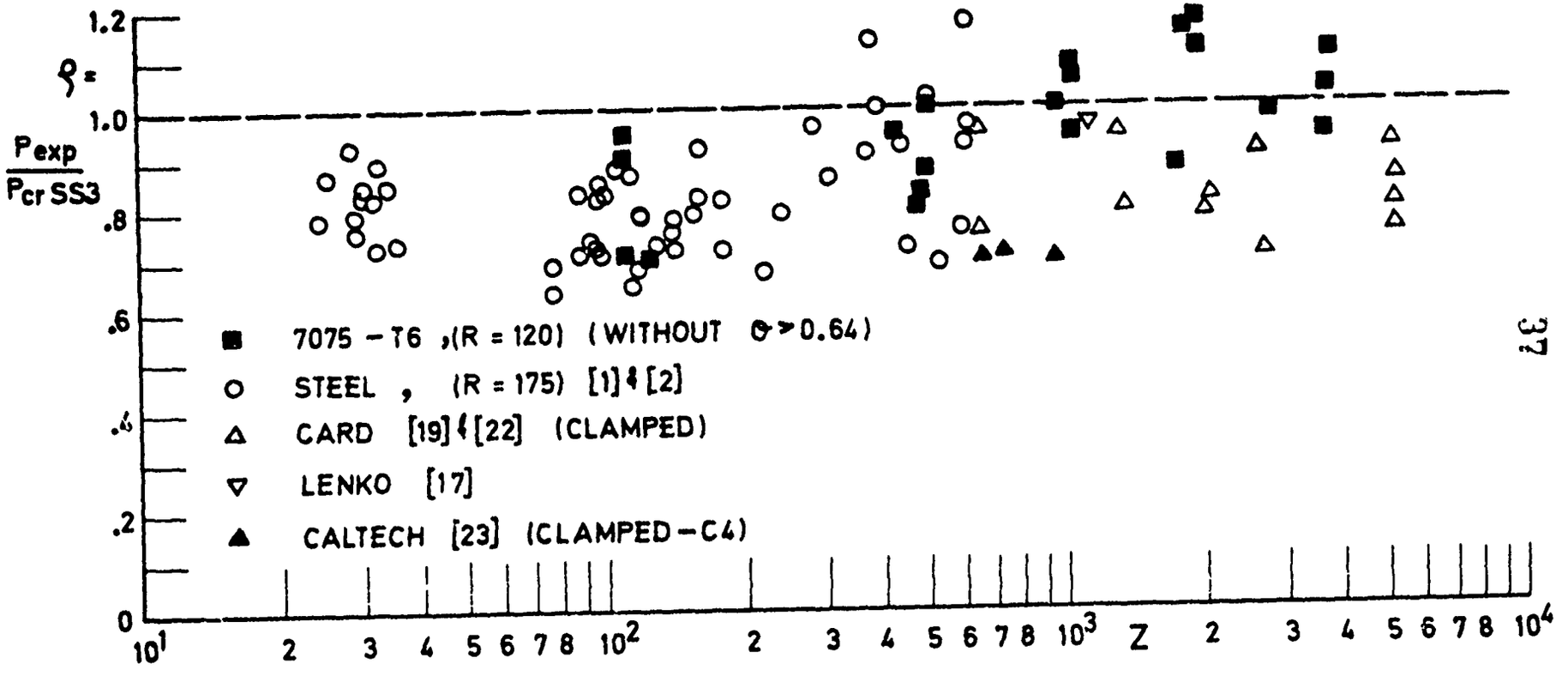

FIG. 12. "LINEARITY" OF STRINGER-STIFFENED SHELLS AS A FUNCTION OF Z (EXCLUDING RESULTS OF [20] AND [21], SMALLER STEEL SHELLS, R=125 AND SHELLS WITH θ>0.64)

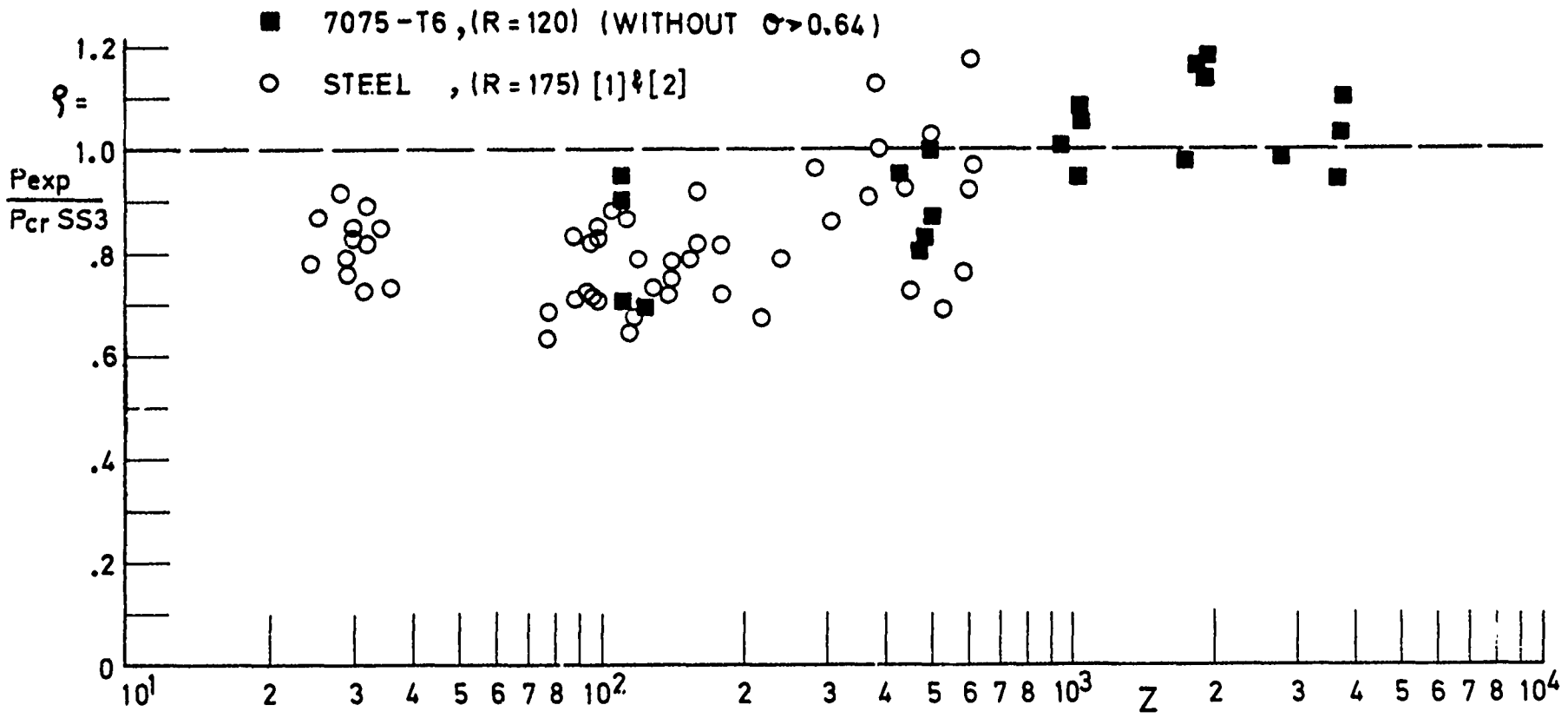

FIG. 15. "LINEARITY" OF 7075-T6 AND STEEL (R=175) STRINGER-STIFFENED SHELLS AS A FUNCTION OF Z (EXCLUDING SHELLS WITH θ>0.64)

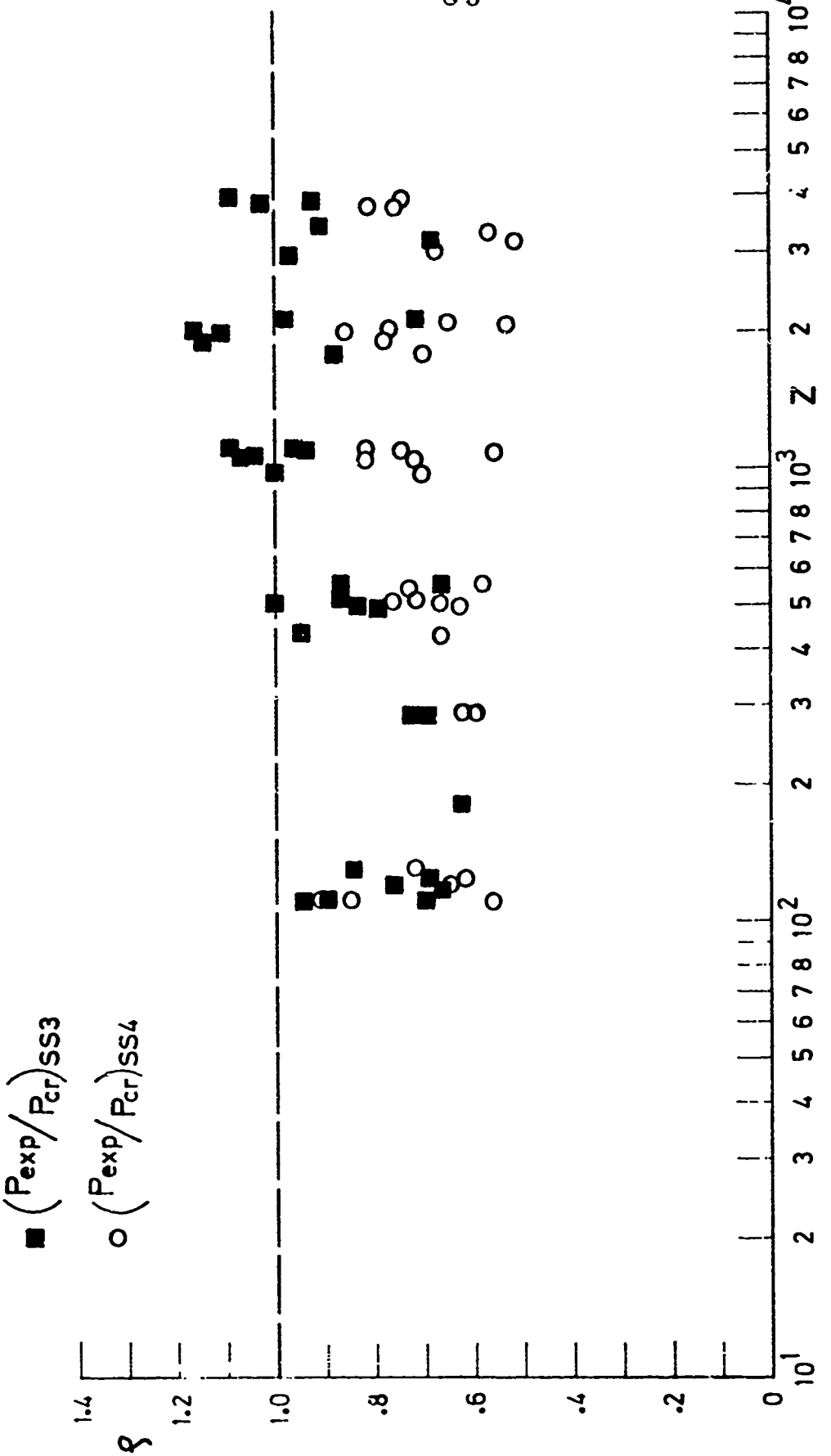

FIG. 14. INFLUENCE OF SS4 BOUNDARY CONDITIONS ON THE "LINEARITY" OF 7075 STRINGER-STIFFENED SHELLS

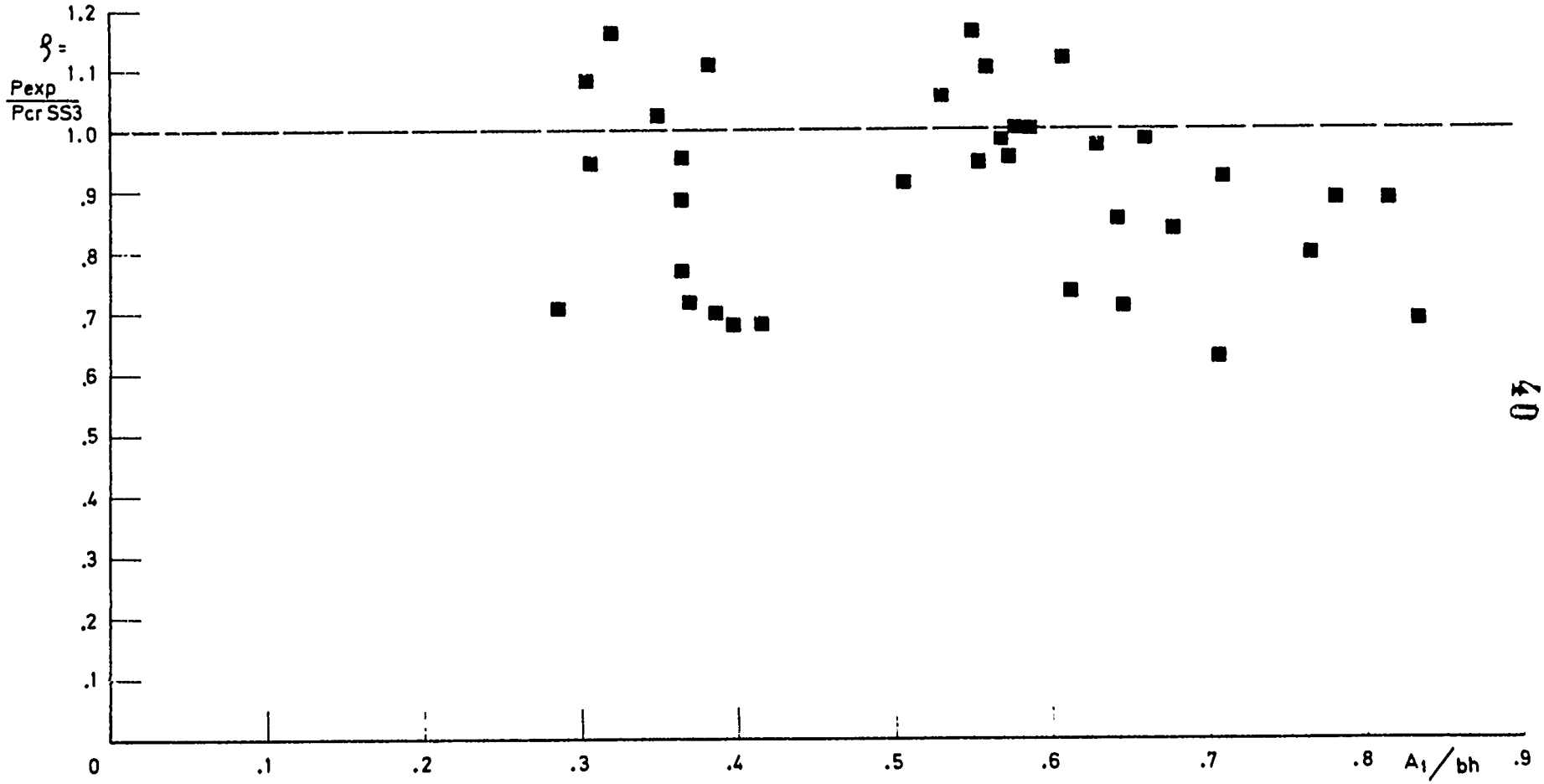

FIG. 15. "LINEARITY" OF 7075-T6 STRINGER-STIFFENED SHELLS AS FUNCTION OF (A_1/bh)

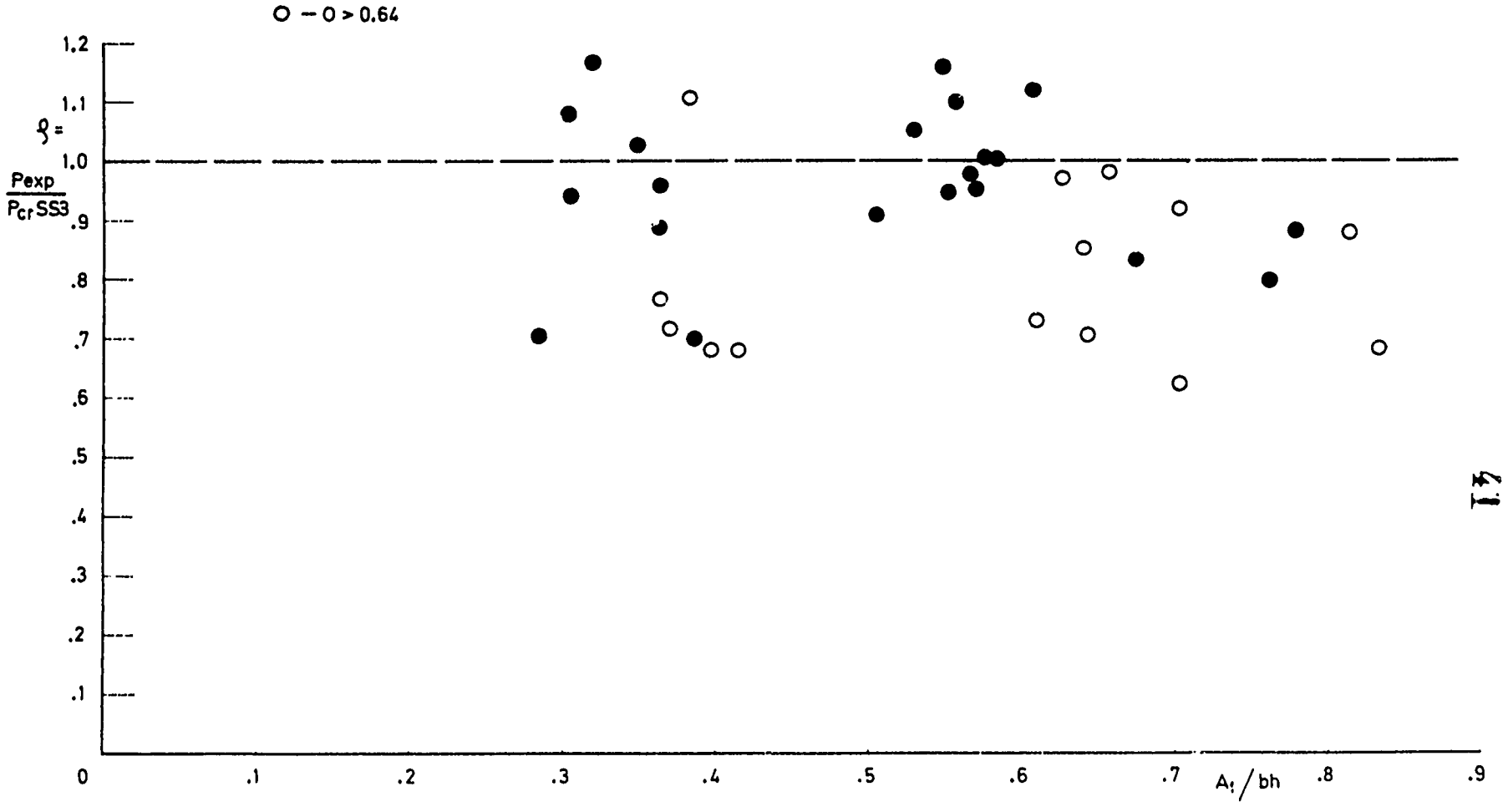

FIG. 16. EFFECT OF UNSTABLE PANEL POSTBUCKLING BEHAVIOR, $\theta > 0.64$ ON "LINEARITY" AS A FUNCTION OF (A_1/bh)

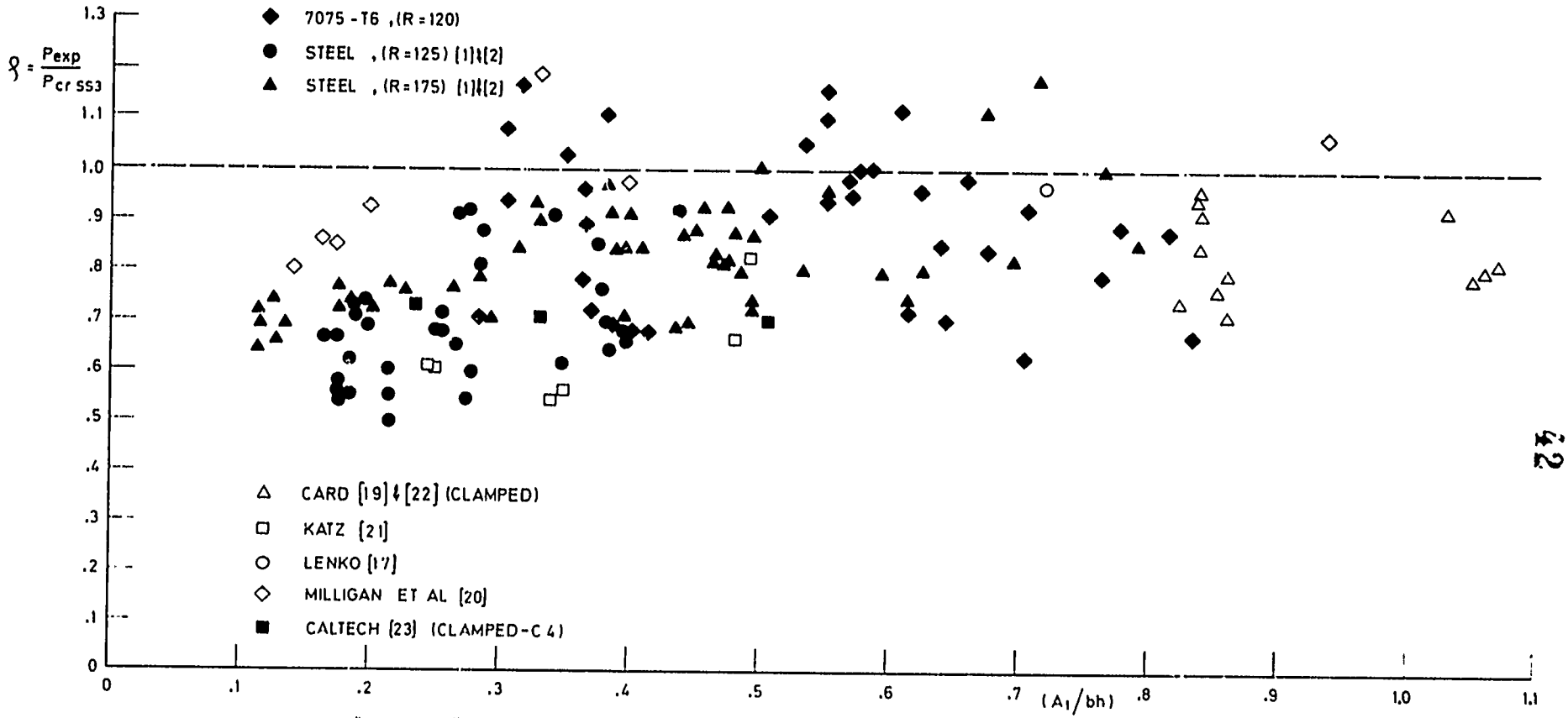

FIG. 17 "LINEARITY" OF STRINGER STIFFENED SHELLS AS A FUNCTION OF (A_1/bh)

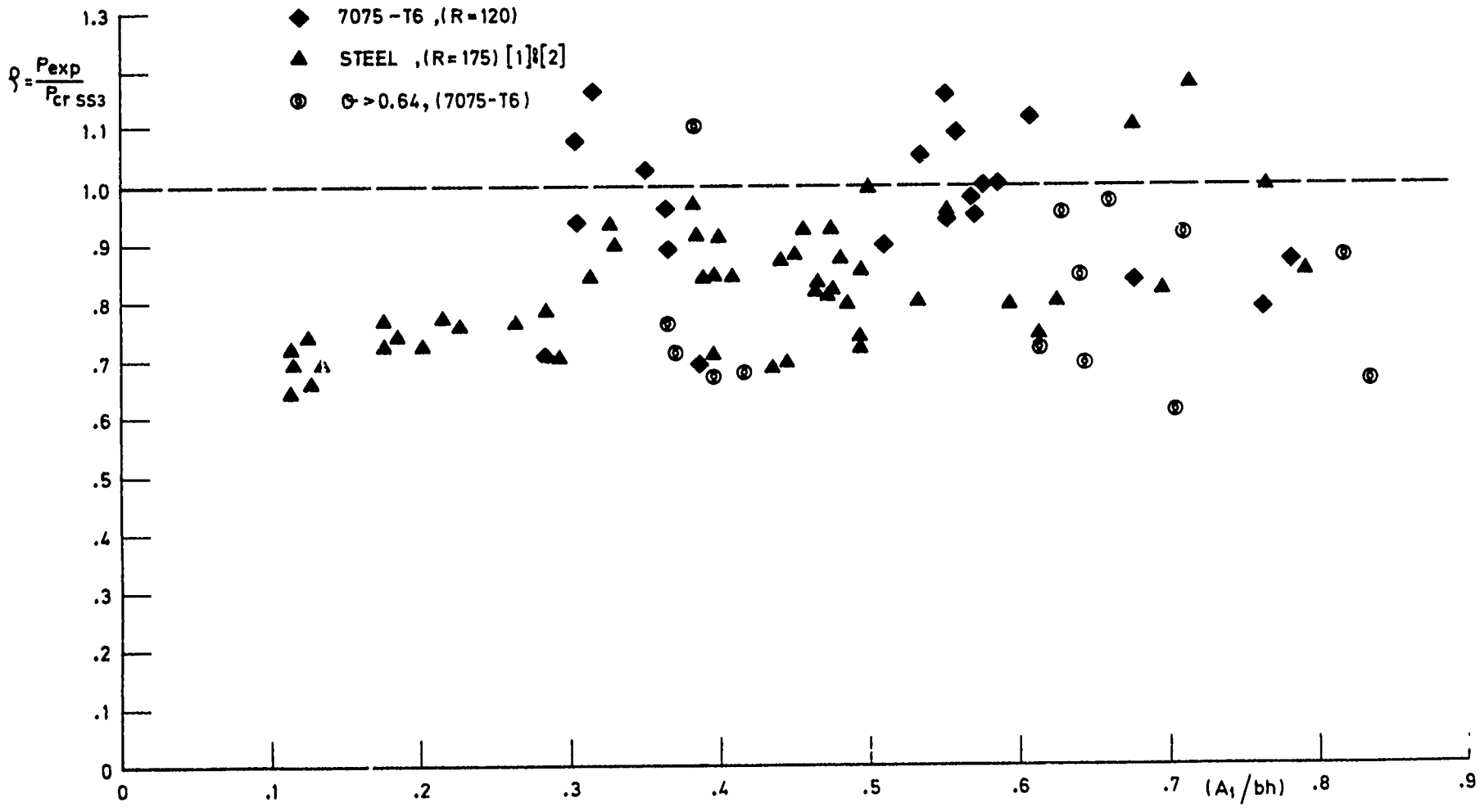

FIG. 18. "LINEARITY" OF 7075-T6 AND LARGER STEEL SPECIMENS AS A FUNCTION OF (A_1/bh)

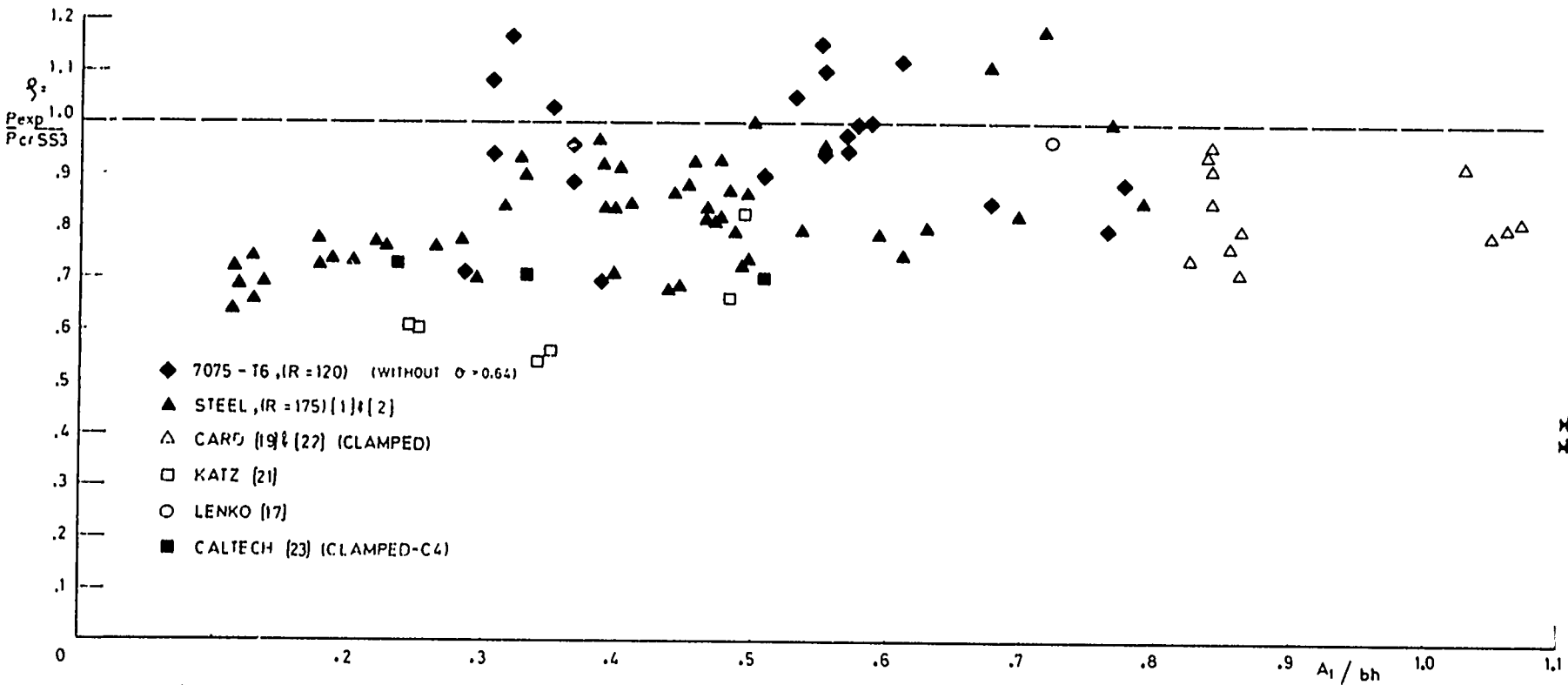

FIG. 19 "LINEARITY" OF STRINGER - STIFFENED SHELLS AS A FUNCTION OF (A_1/bh) (EXCLUDING RESULTS OF [20] SMALLER STEEL SHELLS, R = 125, AND SHELLS WITH $\sigma > 0.64$)

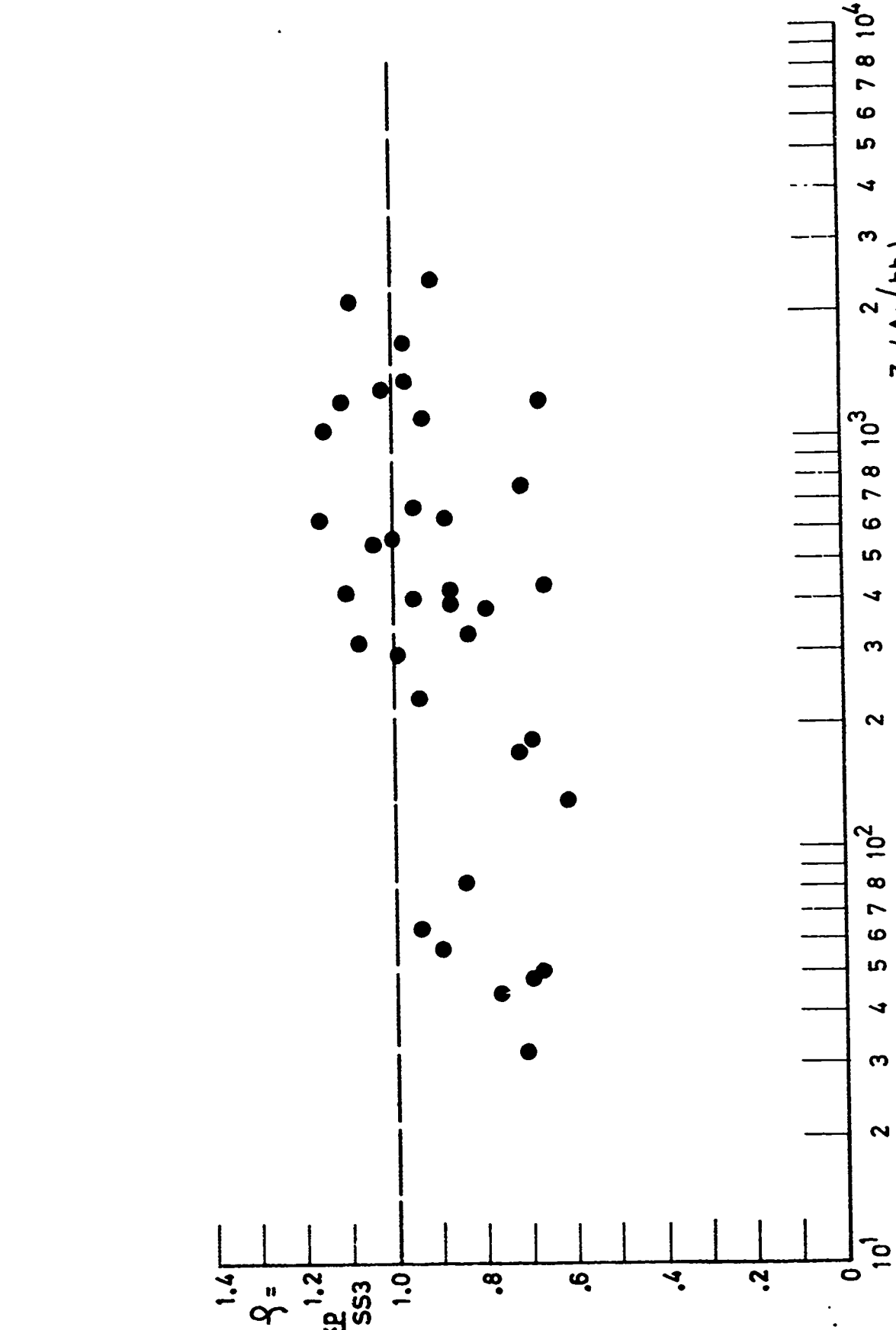

FIG. 20. "LINEARITY" OF 7075-T6 STRINGER-STIFFENED SHELLS AS A FUNCTION OF $Z(A_1/bh)$

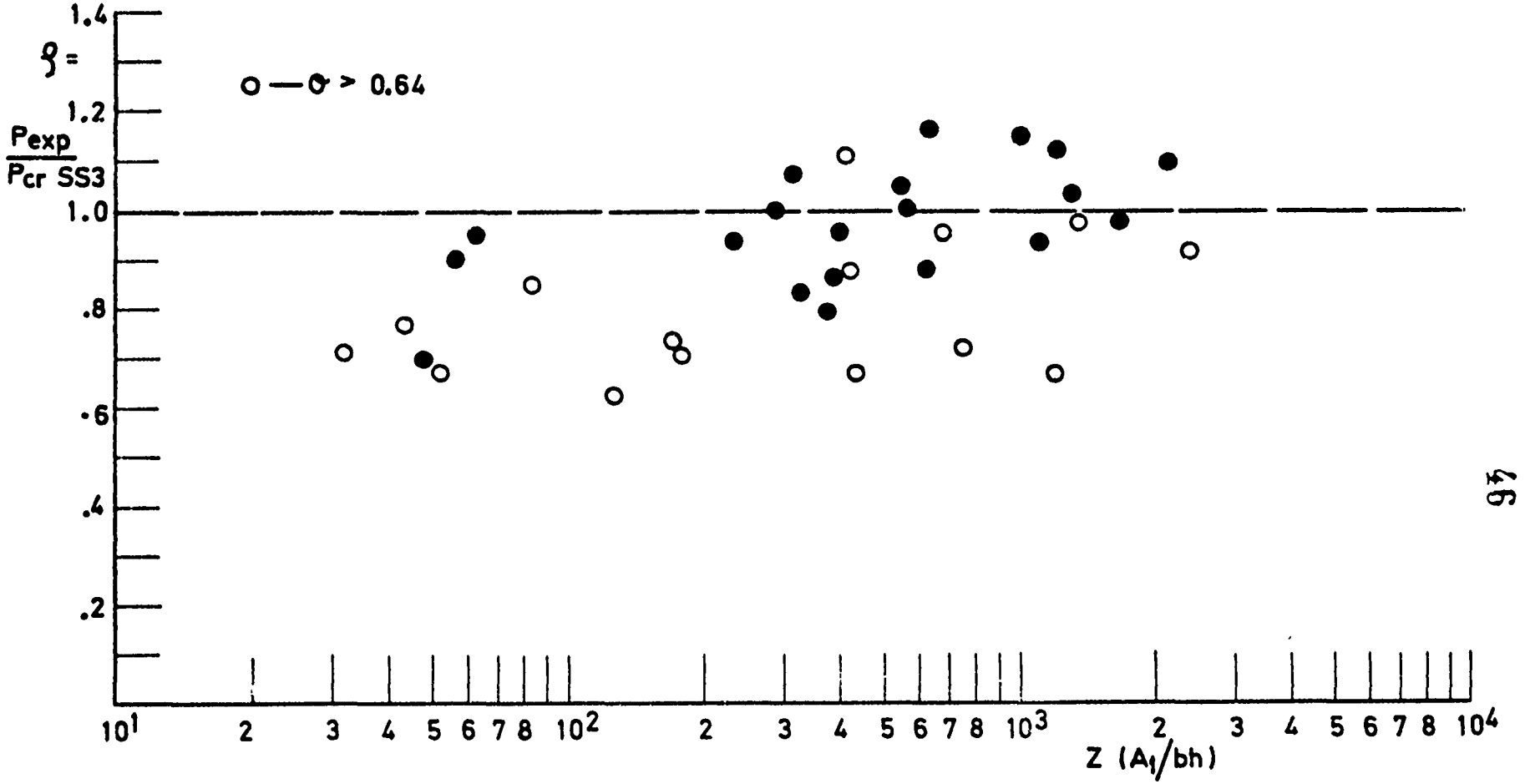

FIG. 21. EFFECT OF UNSTABLE PANEL POSTBUCKLING BEHAVIOR, $\sigma > 0.64$, ON THE "LINEARITY" AS A FUNCTION OF $Z(A_1/bh)$

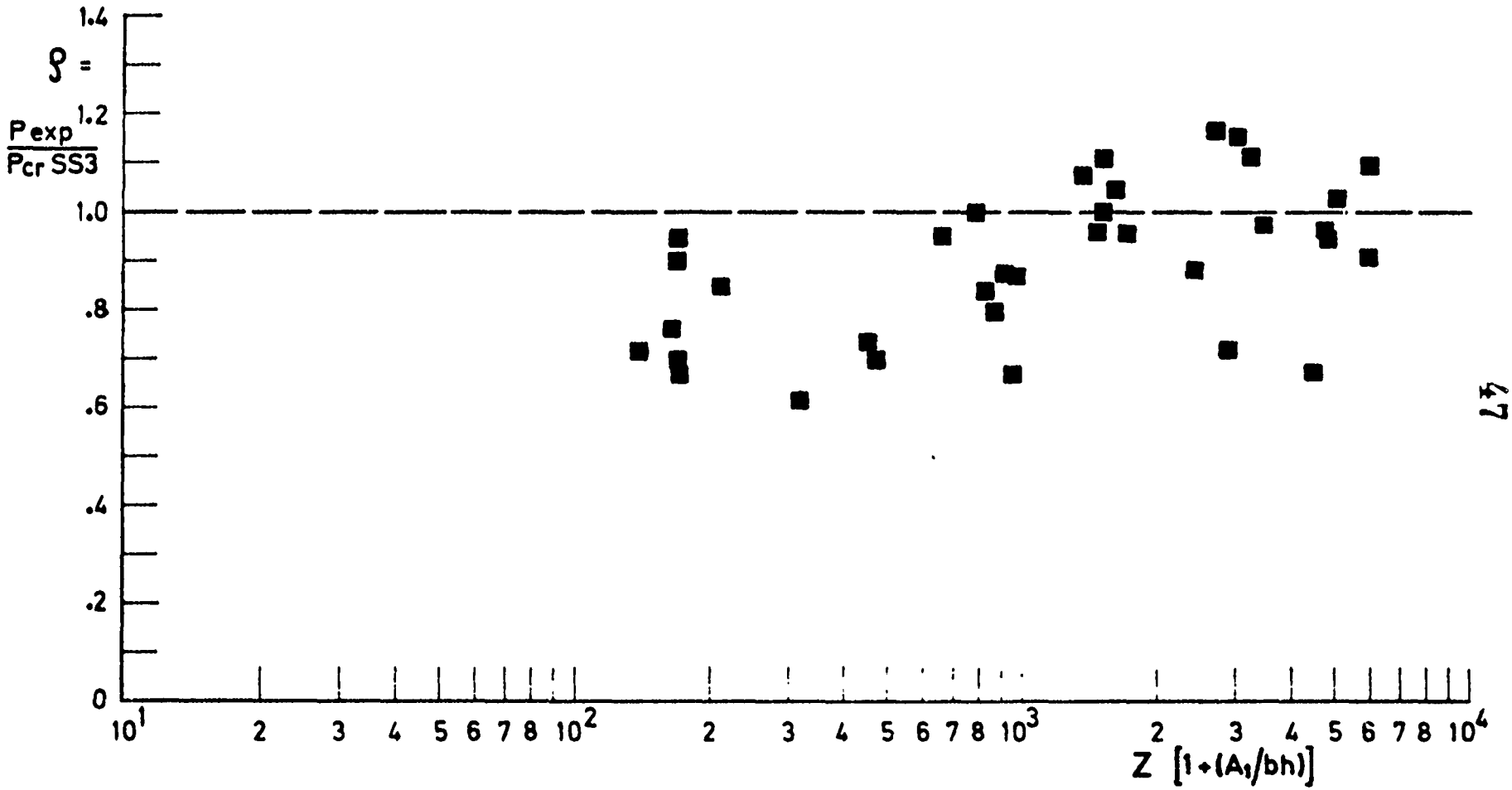

FIG. 22. "LINEARITY" OF 7075-T6 STRINGER-STIFFENED SHELLS AS A FUNCTION OF "WEIGHTED SHELL GEOMETRY" $Z[1+(A_1/bh)]$

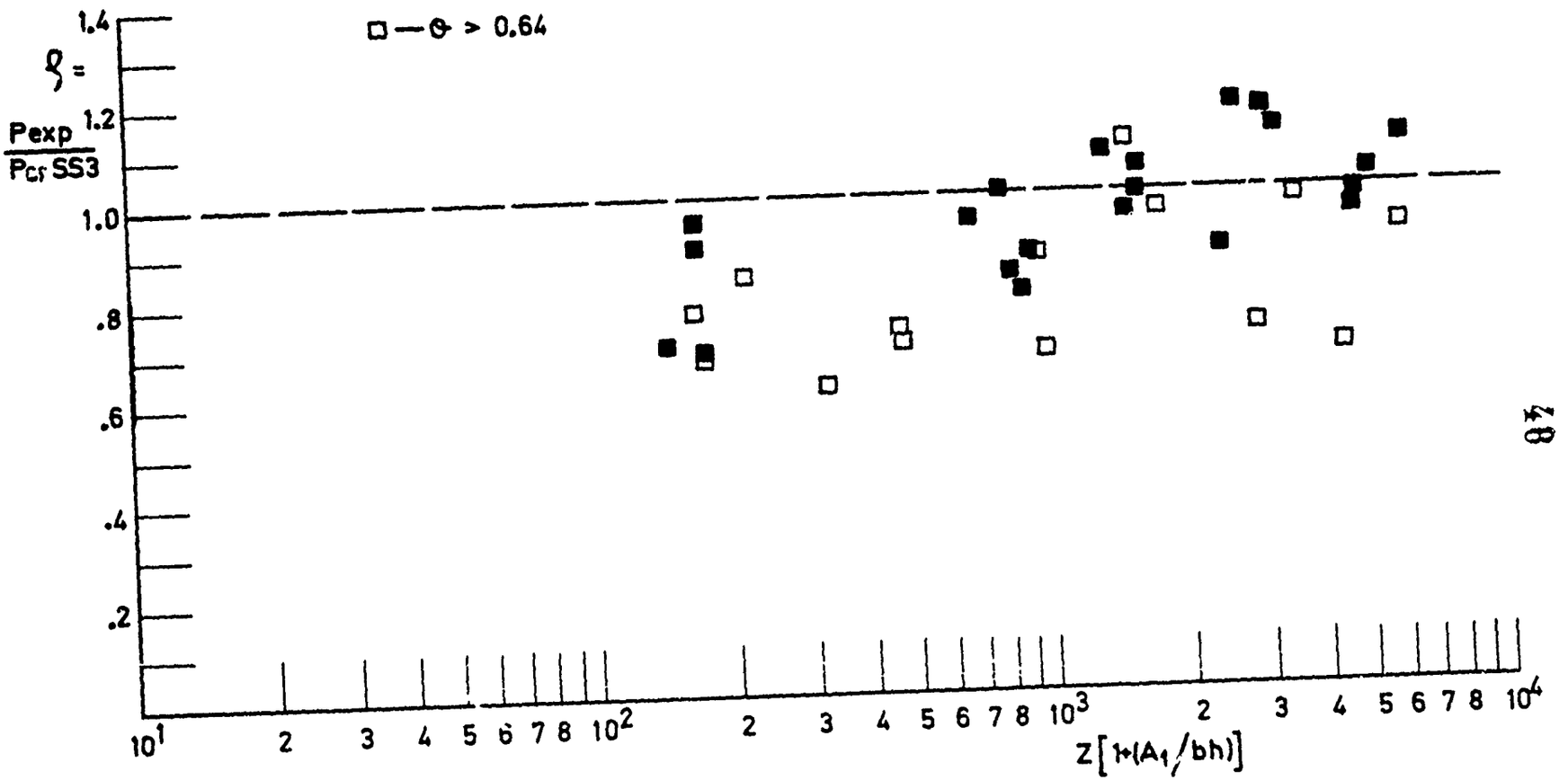

FIG. 24. EFFECT OF UNSTABLE PANEL POSTBUCKLING BEHAVIOR, θ>0.64, ON "LINEARITY" AS A FUNCTION OF $Z[1+(A_1/bh)]$

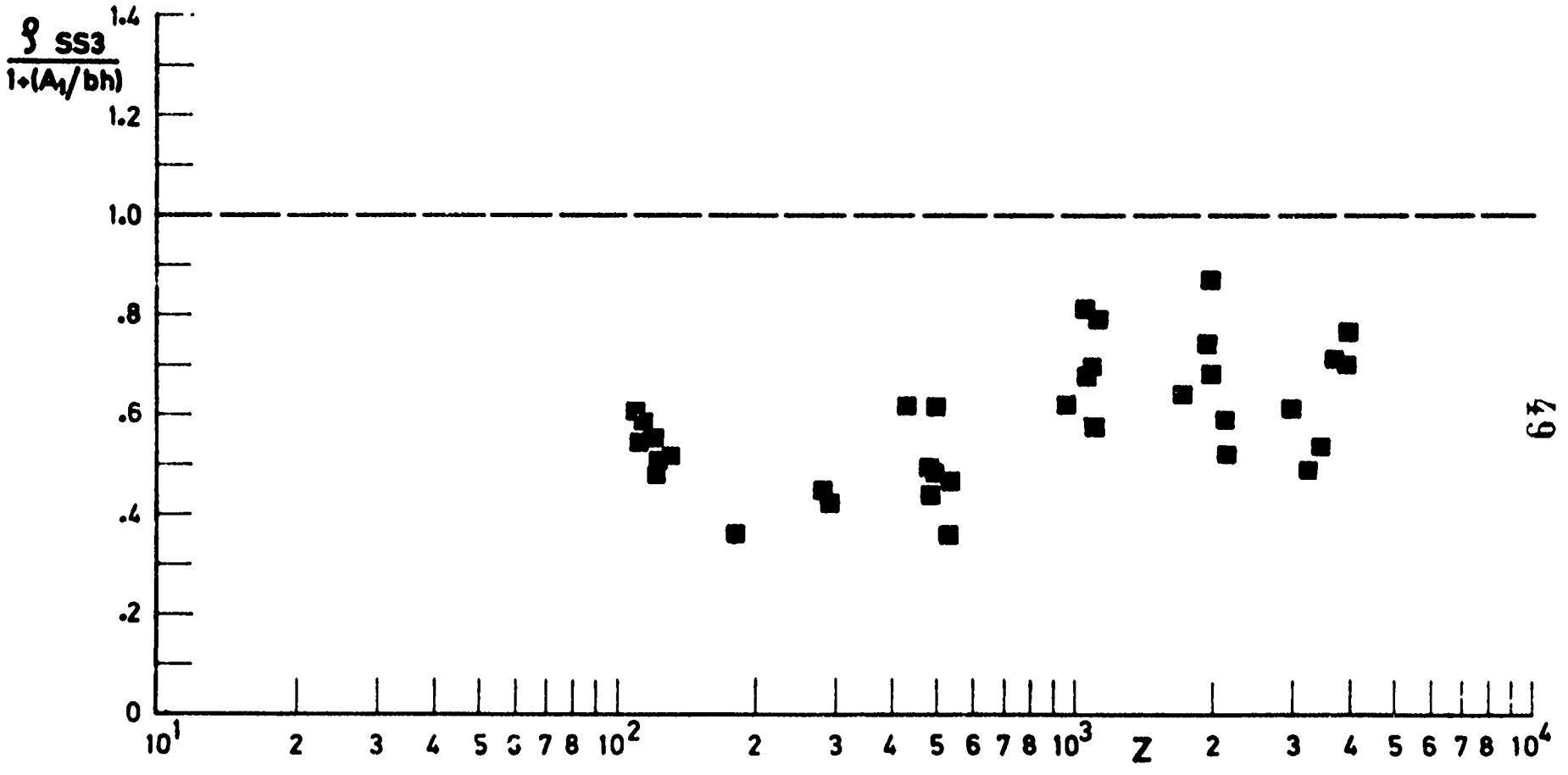

FIG. 24. SS3 " HEIGHT, " CAPACITY" OF 7075-T6 STRINGER-STIFFENED PANELS

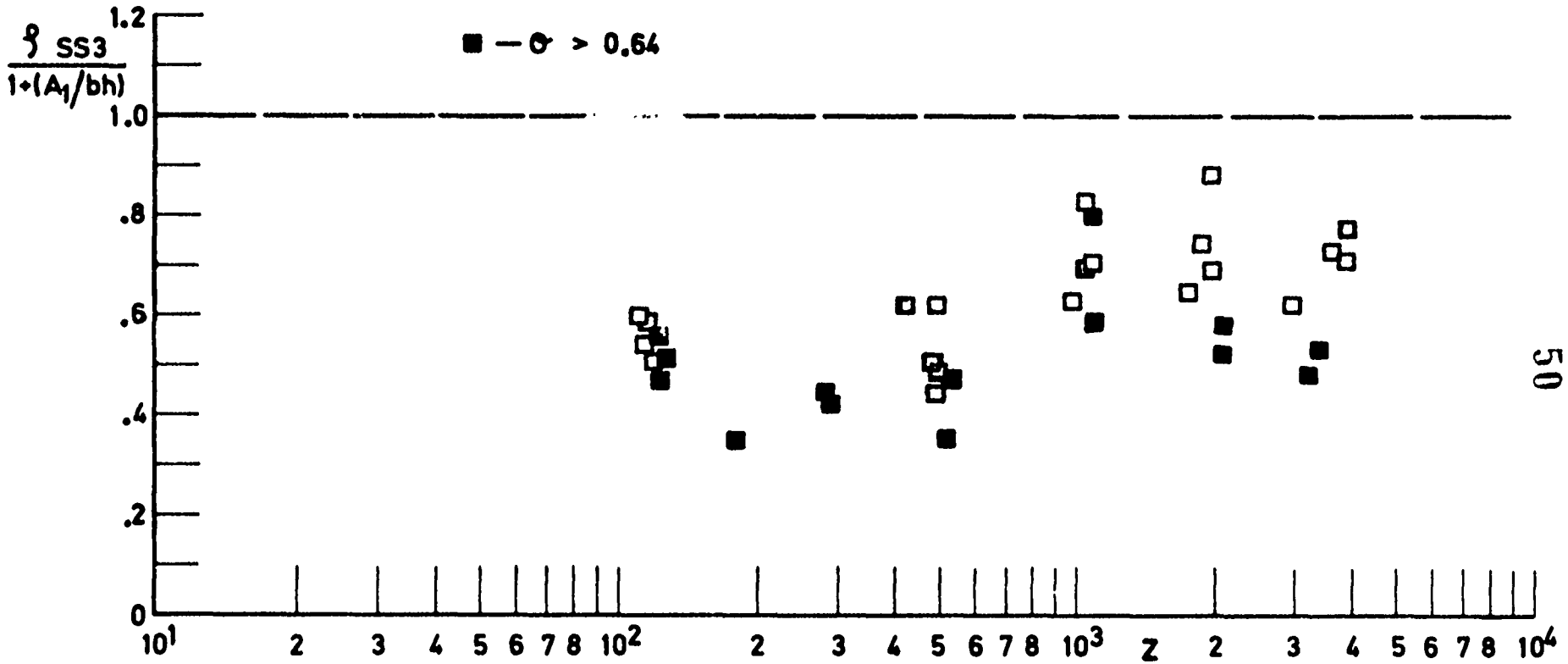

FIG. 25. EFFECT OF UNSTABLE PANEL POSTBUCKLING BEHAVIOR, Θ>0.64, ON SS3 "WEIGHTED LINEARITY"

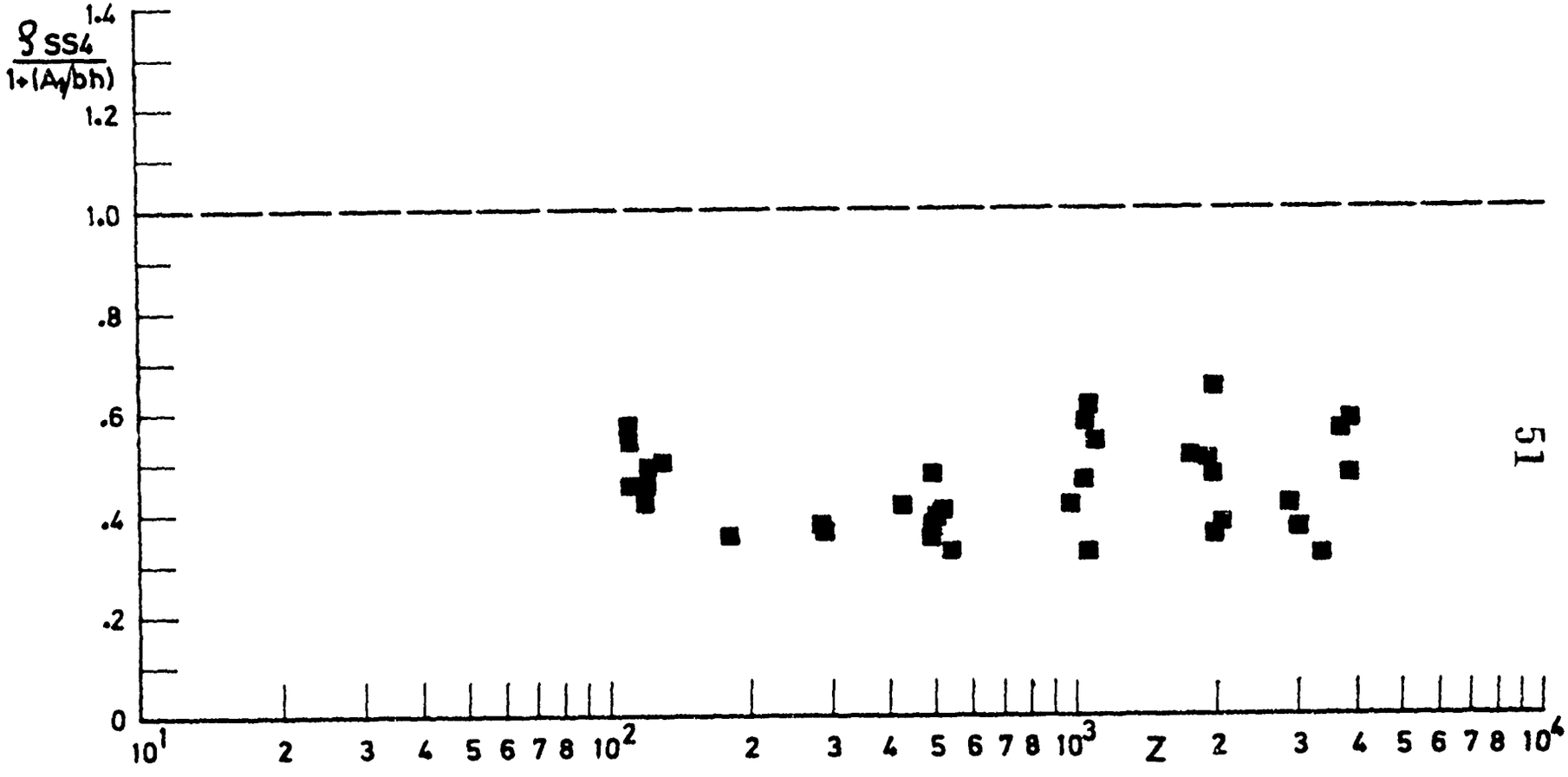

"...LETTED LINEARITY" OF 7075-T6 STRINGER-STIFFENED SHELLS

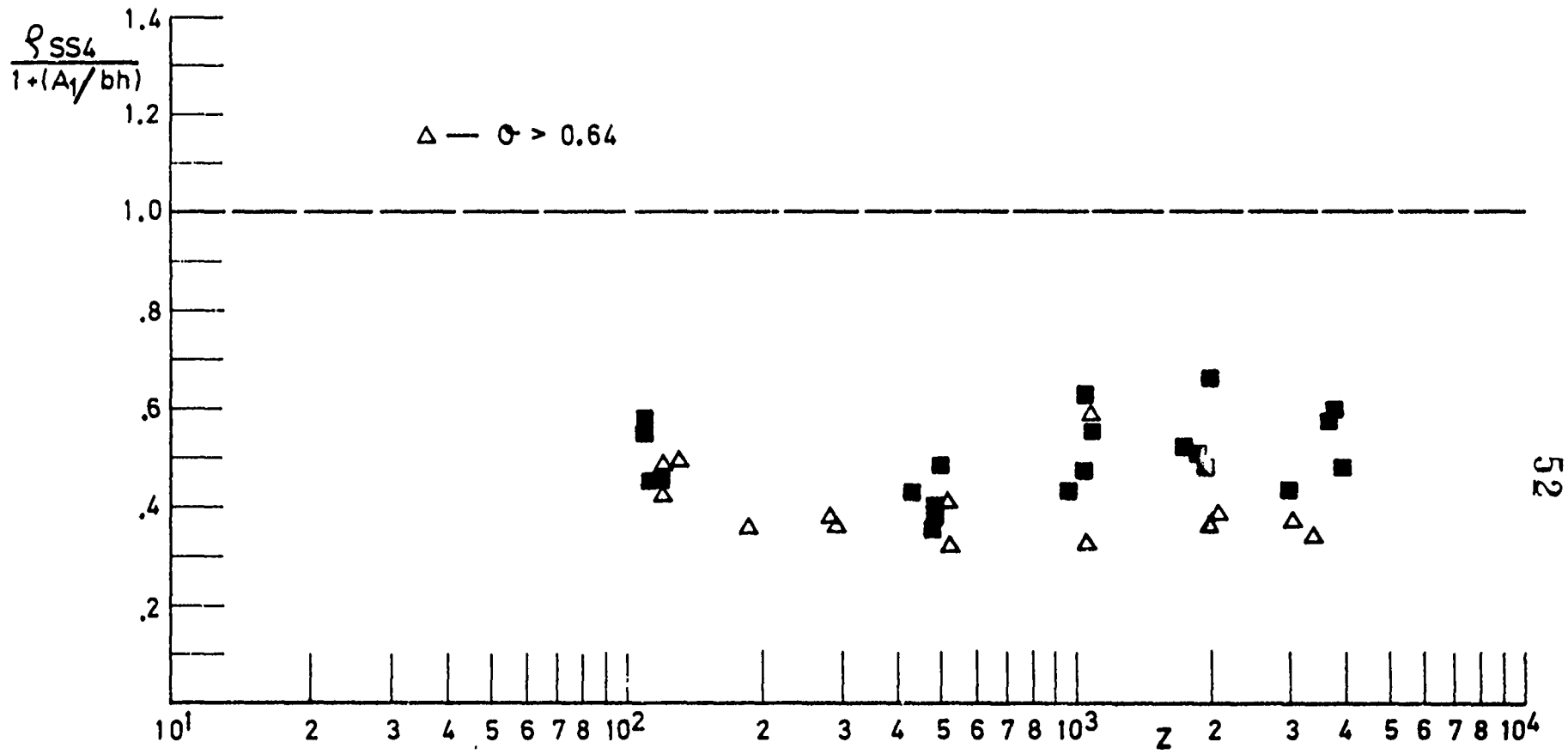

FIG. 27. EFFECT OF UNSTABLE PANEL POSTBUCKLING BEHAVIOR, Θ>0.64, ON SS4 "WEIGHTED LINEARITY"

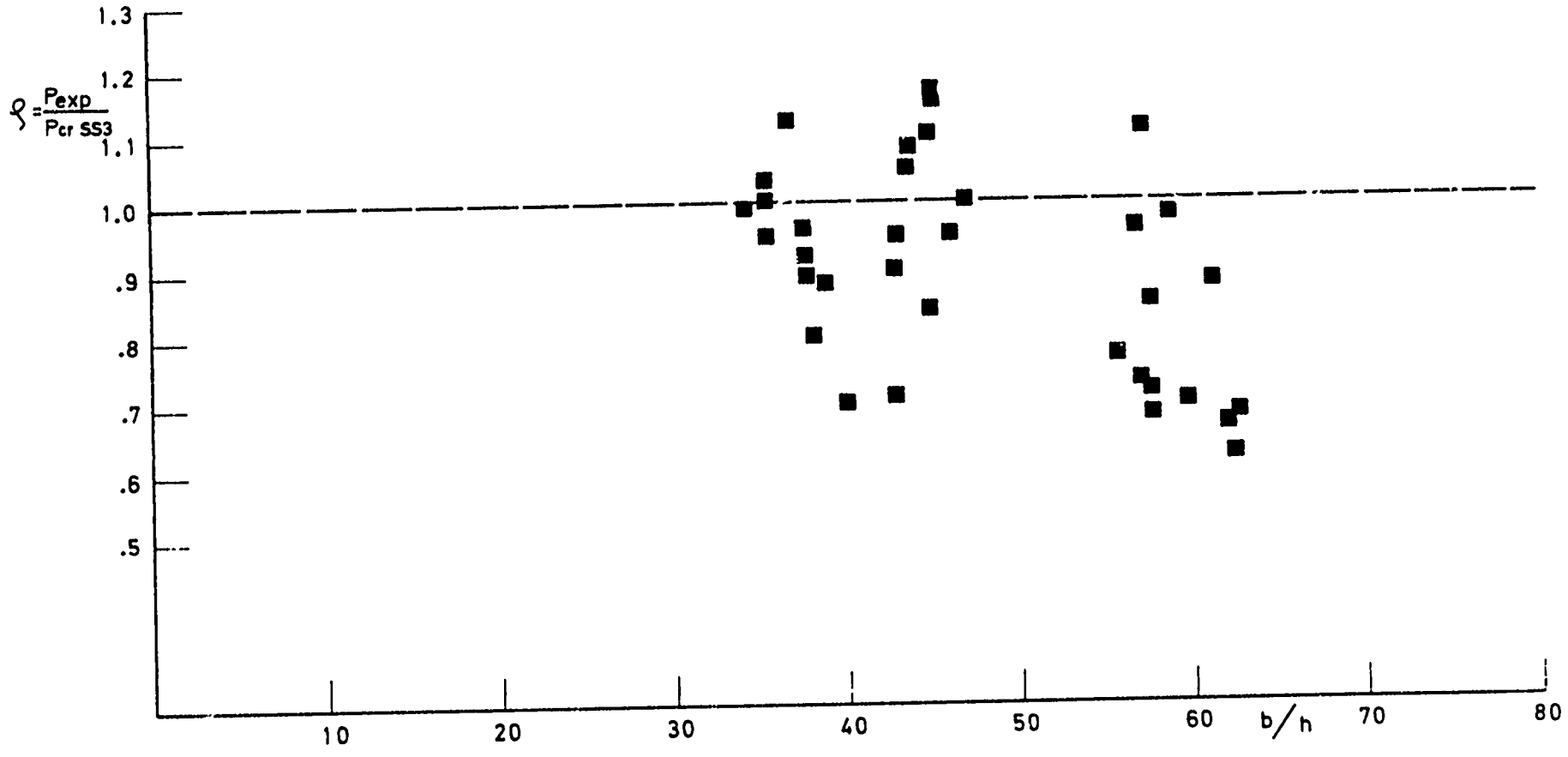

FIG. 28. "LINEARITY" OF 7075-T6 STRINGER-STIFFENED SHELLS AS A FUNCTION OF STRINGER-SPACING, (b/h)

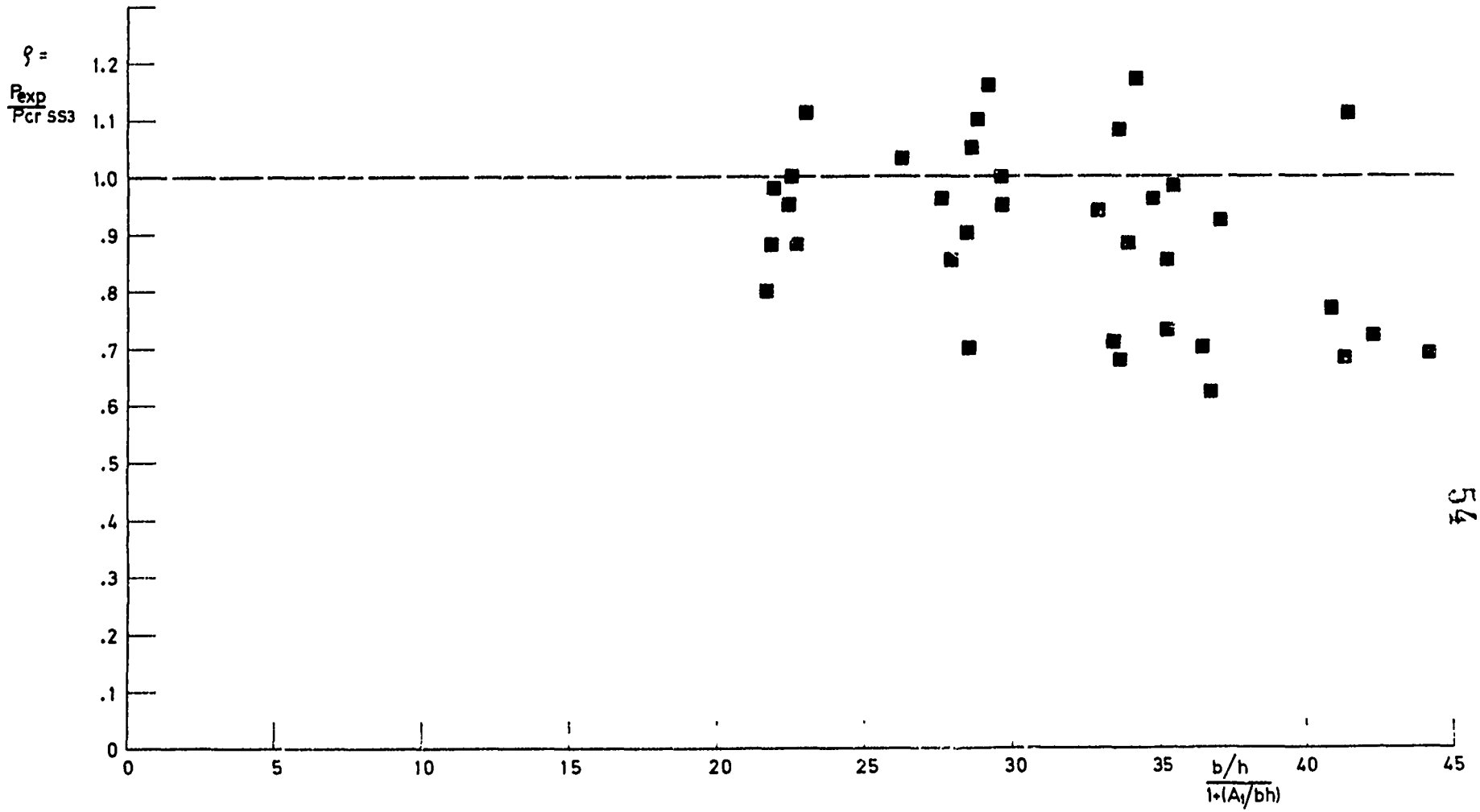

FIG. 29. "LINEARITY" OF 7075-T6 STRINGER-STIFFENED SHELLS AS A FUNCTION OF $(b/h)/[1+(A_1/bh)]$

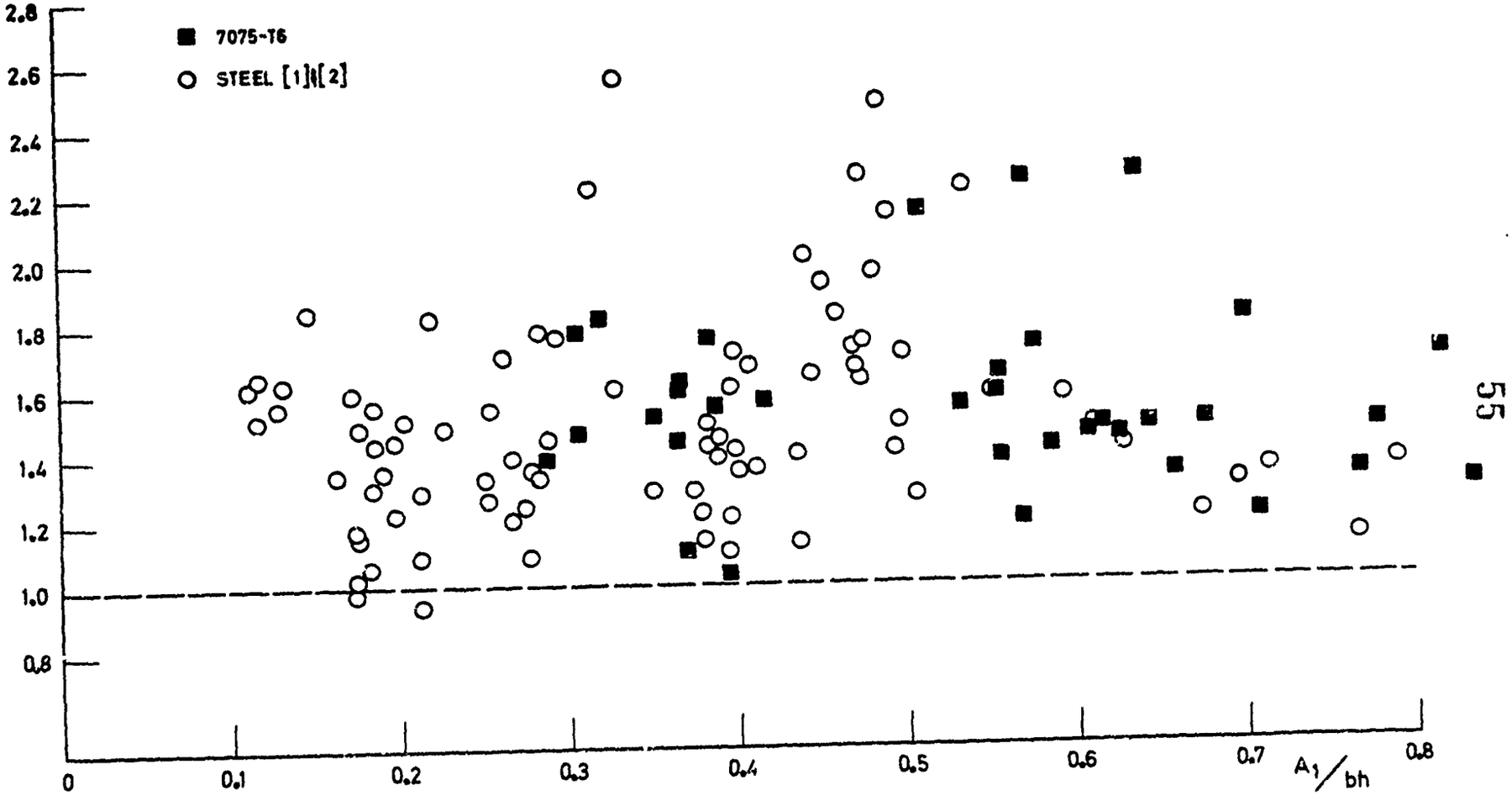

FIG. 30 STUCTURAL EFFICIENCY OF STRINGER-STIFFENED SHELLS

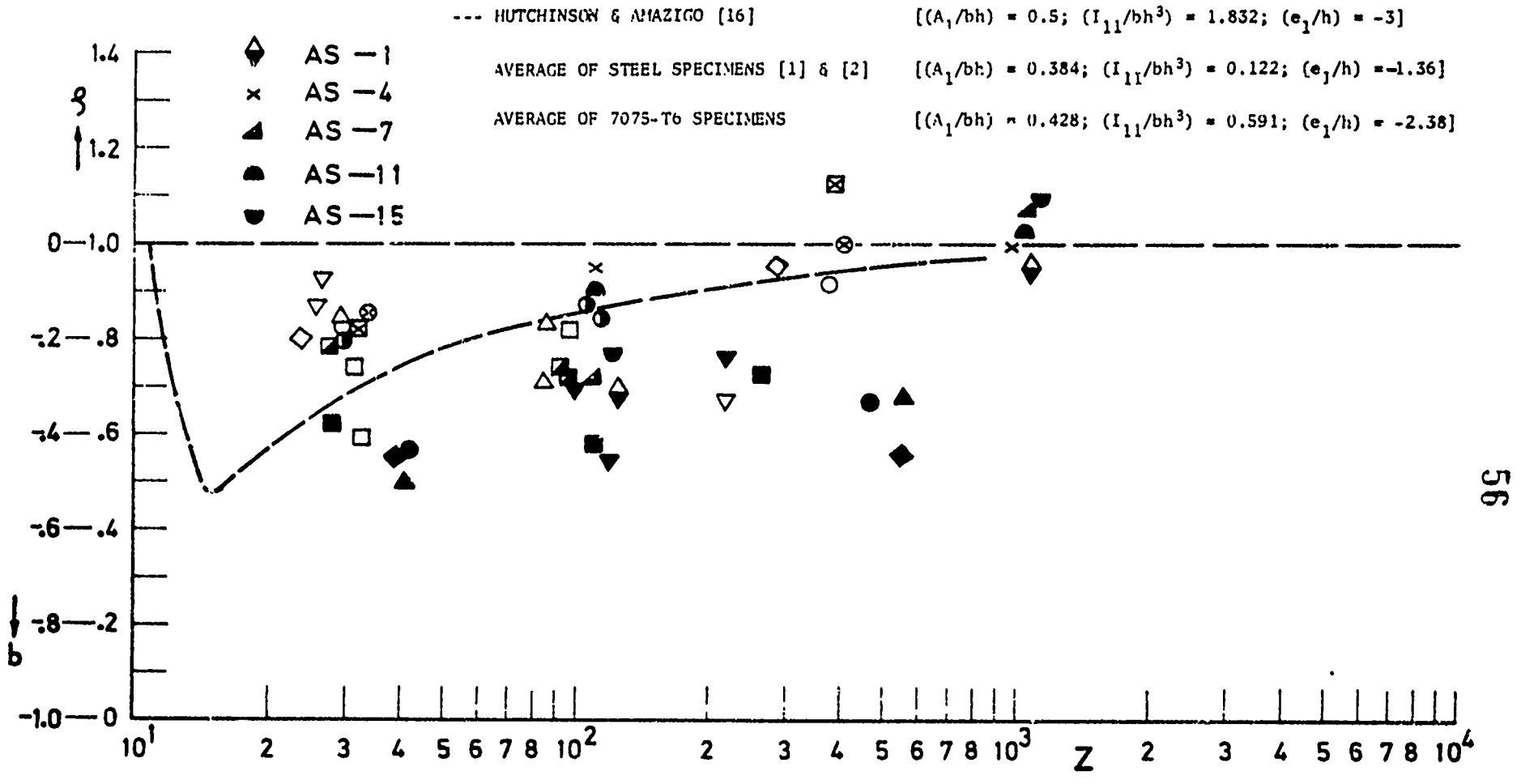

FIG. 31. EXPERIMENTAL CORRELATION STUDY OF IMPERFECTION SENSITIVITY DEPENDENCE ON SHELL GEOMETRY, Z

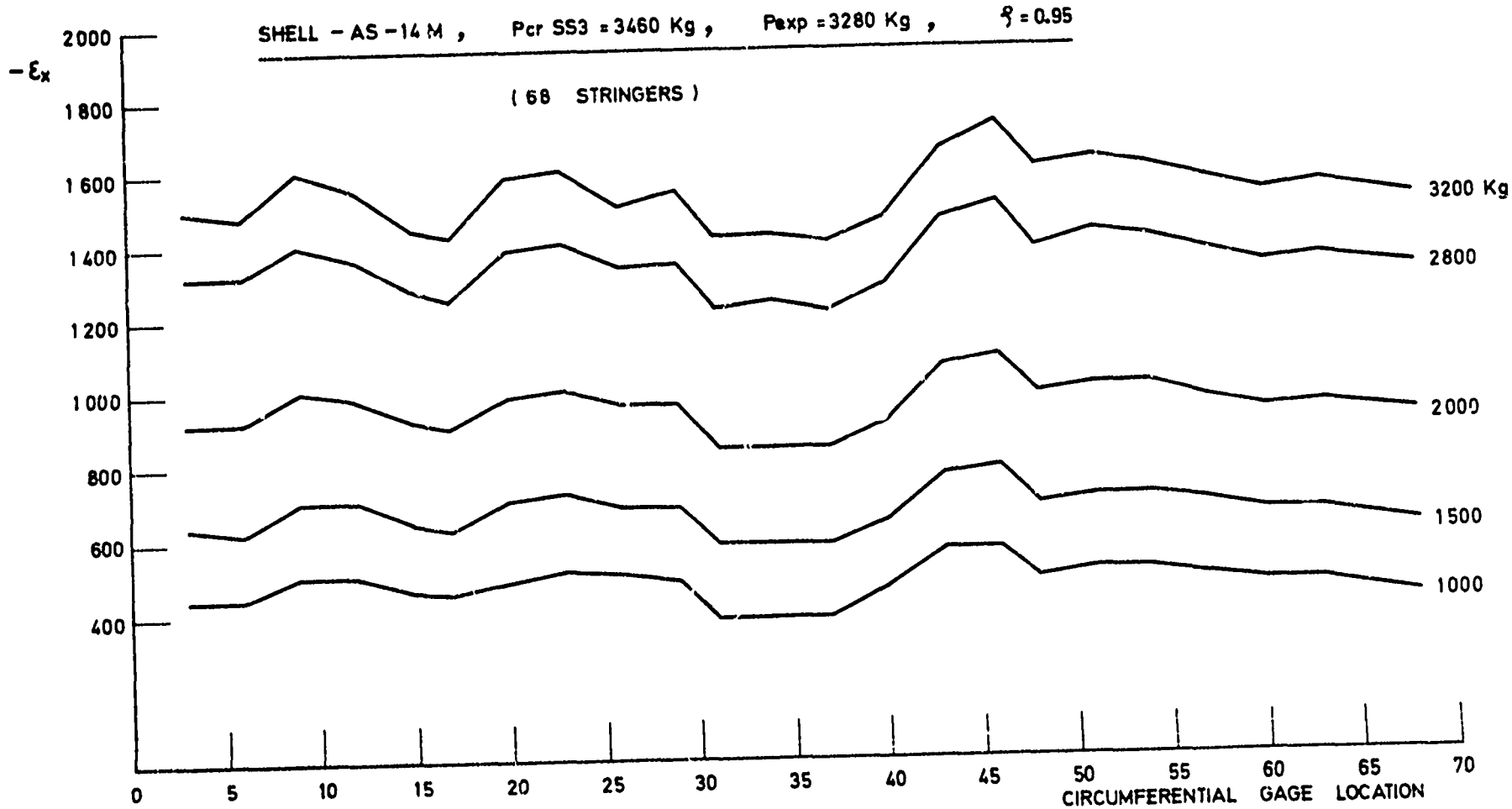

FIG. 32. TYPICAL CIRCUMFERENTIAL DISTRIBUTION OF AXIAL STRAIN (SHELL AS-14M)

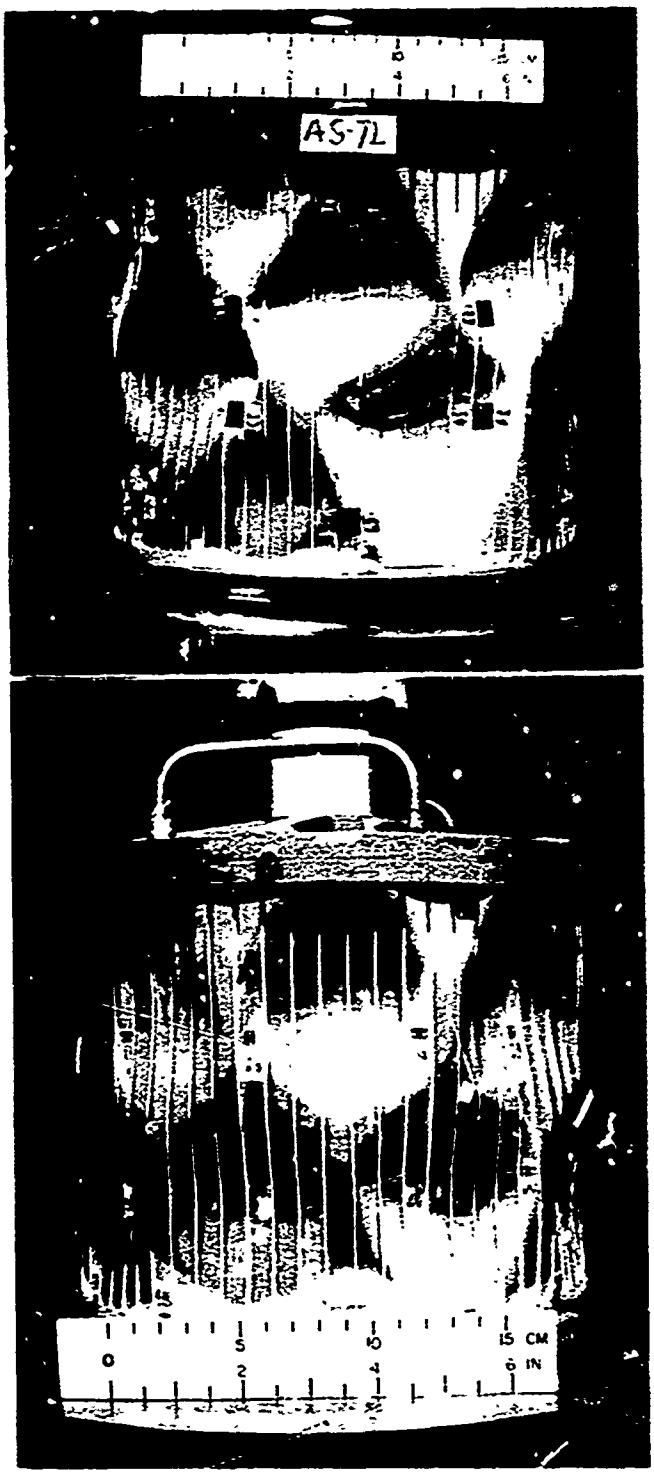

FIG. 33. POSTBUCKLING PATTERNS OF "MEDIUM" LENGTH SPECIMENS

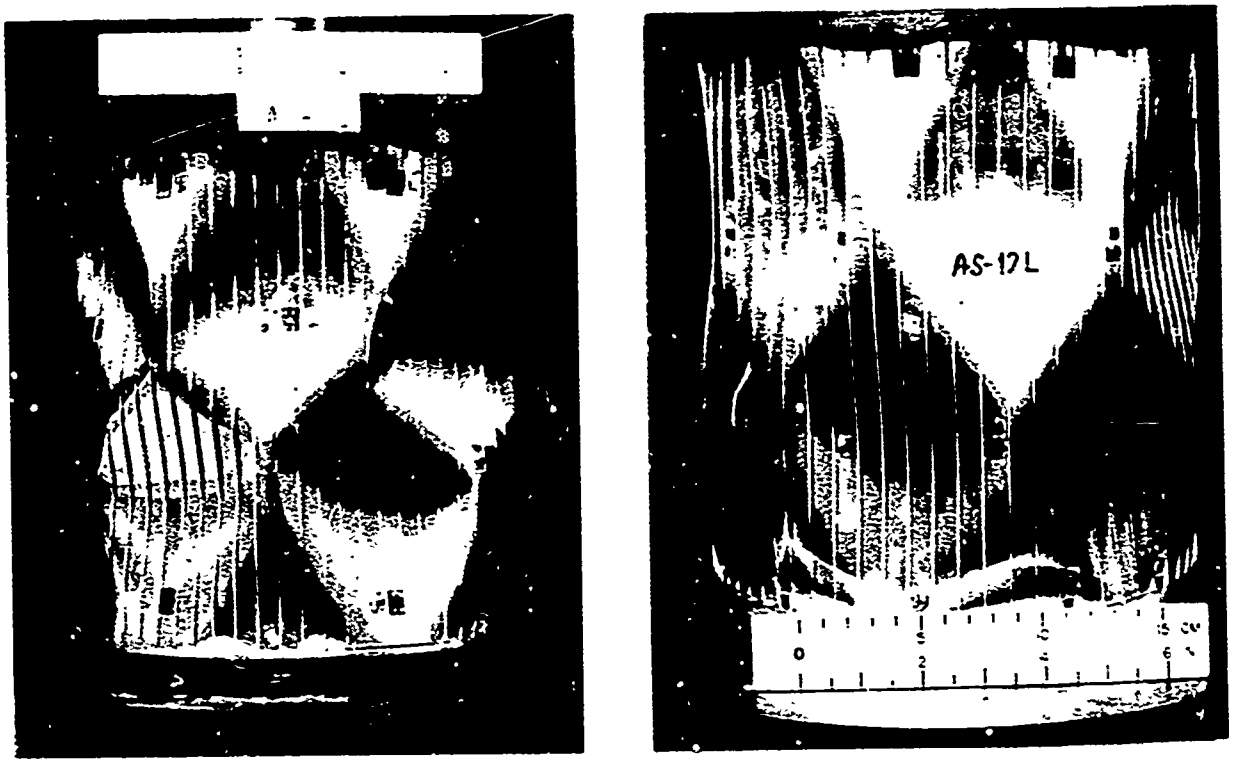

FIG. 34. POSTBUCKLING PATTERNS OF "LONG" SPECIMENS

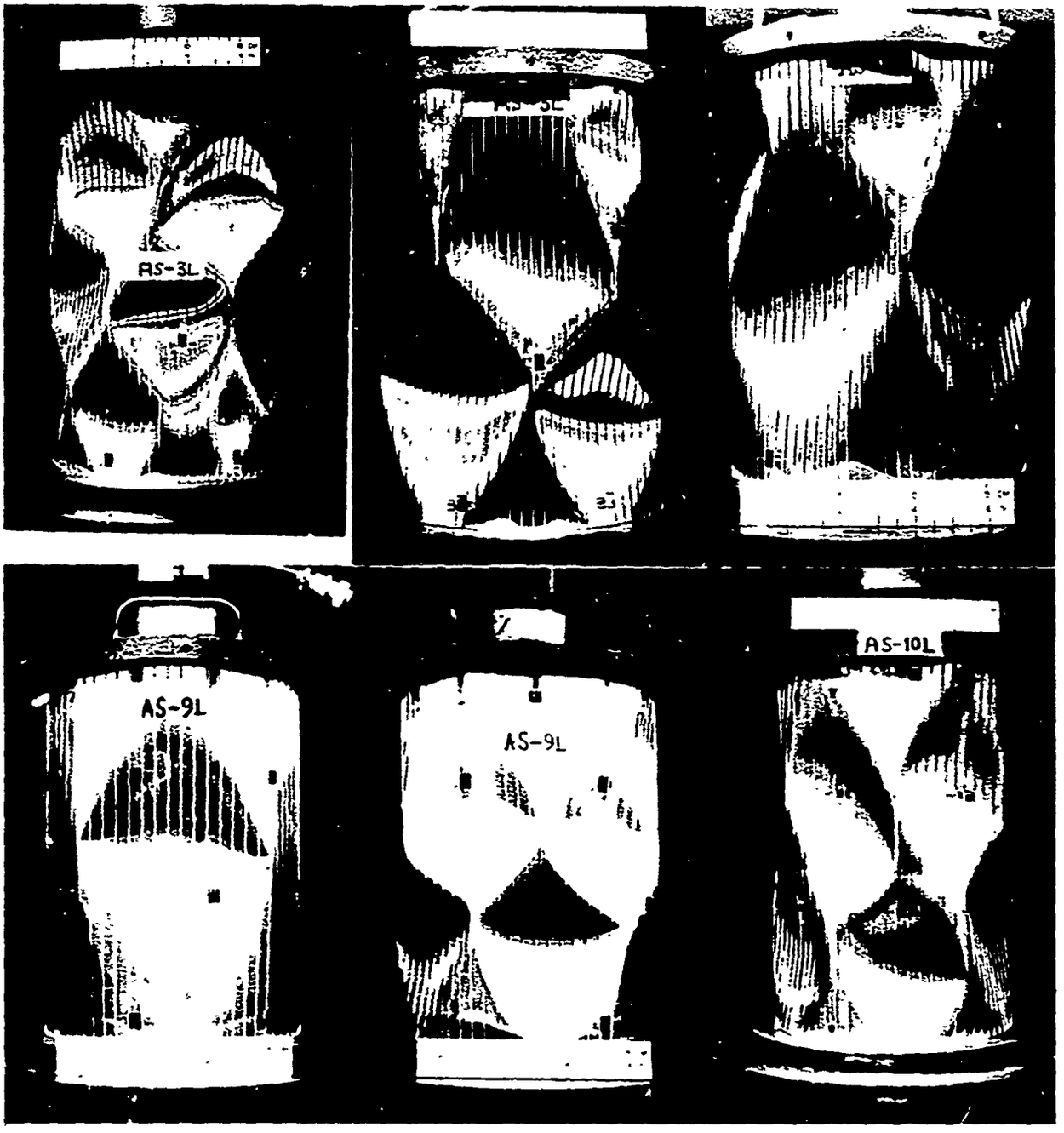

FIG.35. POSTBUCKLING PATTERNS OF "VERY LONG" SPECIMENS

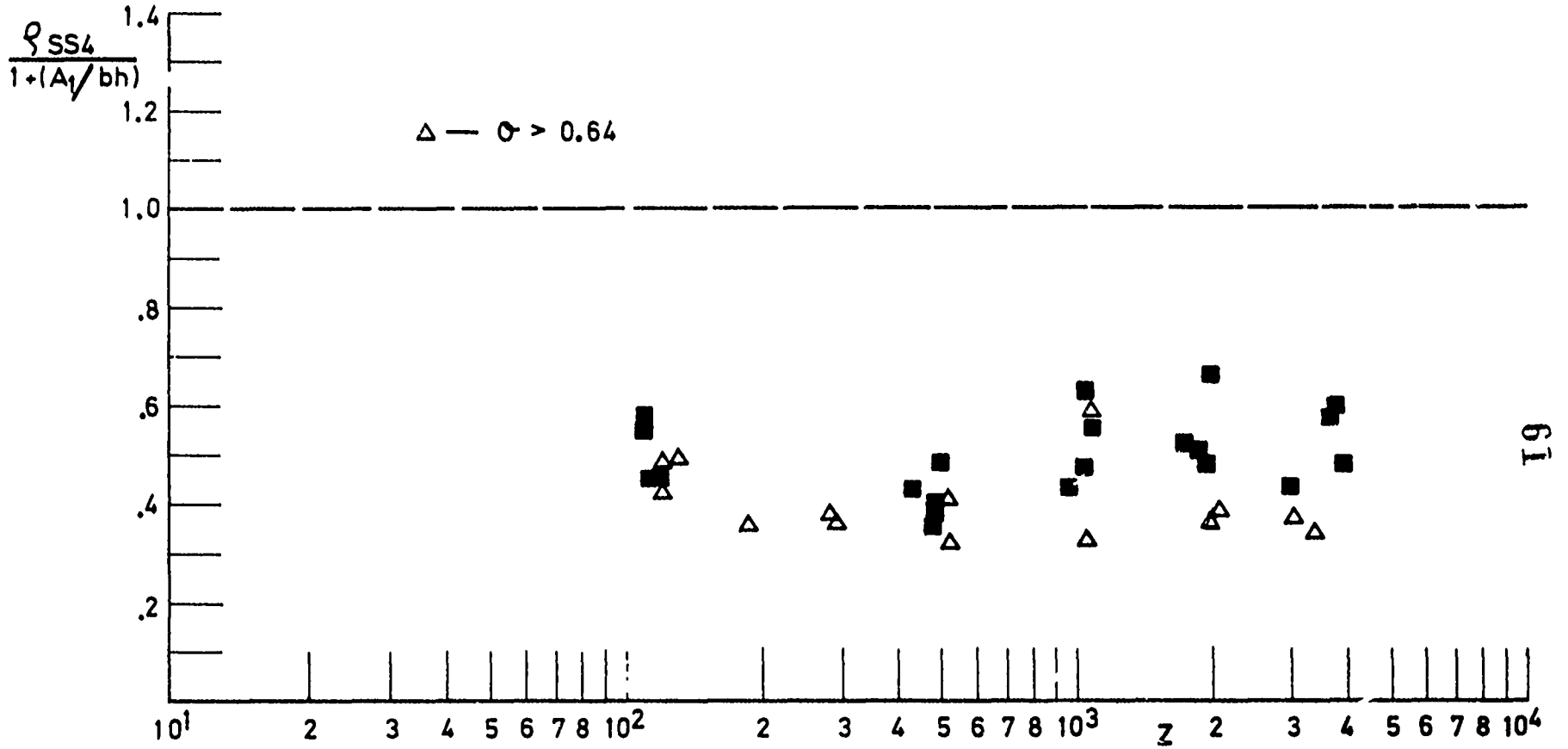

FIG. 27. EFFECT OF UNSTABLE PANEL POSTBUCKLING BEHAVIOR, σ>0.64, ON SS4 "WEIGHTED LINEARITY"